Table 3. Effects of clinical factors on OS in Cox analyses

	All patients (n = 90)						Patients had not received chemotherapy (n = 78)					
	Univariate analysis		Multivariate model A		Multivariate model B		Univariate analysis		Multivariate model C		Multivariate model D	
Clinical factor	HR (95% CI)	P	HR (95% CI)	P	HR (95% CI)	P	HR (95% CI)	P	HR (95% CI)	P	HR (95% CI)	P
PS												
0	1		1		1		1		1		1	
1	1.5 (0.8-2.7)	.22	1.4 (0.8-2.8)	.27	1.3 (0.7-2.6)	.37	1.4 (0.7-2.7)	.28	1.6 (0.8-3.1)	.21	1.4 (0.7-2.9)	.30
2 or more	2.5 (1.2-5.2)	.01	2.1 (1.0-4.6)	.06	2.1 (1.0-4.6)	.06	1.7 (0.7-4.0)	.26	1.5 (0.6-3.8)	.39	1.6 (0.6-4.2)	.30
Neutrophil counts												
Less than 7.5×10^9/L	1		1		1		1		1		1	
7.5×10^9/L or greater	1.6 (0.9-2.9)	.15	1.3 (0.6-2.7)	.45	1.2 (0.6-2.3)	.58	1.3 (0.6-2.7)	.47	1.5 (0.6-3.8)	.43	1.0 (0.5-2.3)	.94
LDH												
Less than or equal to NI	1		1		1		1		1		1	
Greater than NI	1.7 (1.0-2.9)	.04	1.5 (0.8-2.7)	.16	1.5 (0.8-2.6)	.21	1.5 (0.8-2.8)	.19	1.7 (0.9-3.3)	.12	1.6 (0.8-3.1)	.20
No. of extranodal lesions												
0-2	1		1				1		1			
3 or more	1.5 (0.8-2.8)	.16	0.7 (0.3-1.6)	.41			0.9 (0.4-2.2)	.82	0.5 (0.1-1.6)	.22		
No. of total involved lesions												
1	1				1		1				1	
2 or 3	1.2 (0.7-2.2)	.52			0.8 (0.4-1.6)	.52	1.1 (0.6-2.1)	.67			0.9 (0.4-1.7)	.65
4 or more	1.5 (0.7-3.0)	.26			0.9 (0.4-2.1)	.83	1.0 (0.5-2.3)	.96			0.8 (0.3-2.0)	.67
Chemotherapy												
Not received	1		1		1							
Received	2.6 (1.4-5.1)	.003	2.3 (1.1-4.7)	.03	2.0 (1.0-4.2)	.06						

HR indicates hazard ratio; 95% CI, 95% confidence interval; and NI, normal index.

with more than 3 extranodal lesions was significantly poor than the others ($P = .005$; Figure 2E). The survival rate was worse in patients with more than 4 total involvement lesions than in the others (Table 2). Of the extranodal lesions, we additionally examined the effect of skin lesion and BM involvement on survival rates. The survival rate of patients with BM involvement was significantly poor than of patients without ($P = .04$; data not shown), but that of patients with skin involvement was not different from those without ($P = .66$; supplemental Figure 2).

Although most patients in this study had not been treated until their disease progression was similar to B-cell chronic lymphoid leukemia, 12 patients with chronic ATL were treated with chemotherapy immediately after diagnosis because of elevated LDH levels in 8 patients, severe BM involvement in 2 patients, and severe skin involvements in 2 patients. Among them, 2 patients were treated with VCAP (vincristine, cyclophosphamide, doxorubicin, and prednisone)–AMP (doxorubicin, ranimustine, and prednisone)–VECP (vindesine, etoposide, carboplatin, and prednisone),[3] 2 with CHOP (cyclophosphamide, doxorubicin, vincristine, and prednisone), 4 with CHOP-like, 3 with VEPA (vincristine, etoposide, prednisone, and doxorubicin),[15] and 1 with low-dose etoposide. All of these patients died (MST, 1.4 years; 95% CI, 1.1-2.3 years), and their prognosis was very poor compared with patients not treated ($P = .01$; Figure 2F).

On the basis of results from Kaplan-Meier curves and univariate analysis for each factor, we decided to include PS category, dichotomized neutrophil counts, dichotomized LDH category, dichotomized number of extranodal lesions, the number of total involved lesions, and chemotherapy states into multivariate Cox analysis. Model A included PS category, dichotomized neutrophil counts, dichotomized LDH category, dichotomized number of extranodal lesions, and chemotherapy states. Model B included the same factors as model A except for the number of total involved lesions instead of the number of extranodal lesions. This was because, by definition, a factor of the number of total involved lesions included a factor of the number of extranodal lesions. Results were summarized in Table 3. In model A, advanced PS (≥ 2; HR, 2.1; 95% CI, 1.0-4.6; $P = .06$, borderline significance) and chemotherapy states (HR, 2.3; 95% CI, 1.1-4.7; $P = .03$, significance) were correlated with OS, but the remaining factors were not independent prognostic factors after adjustment for covariate factors. To evaluate effects of clinical factors beyond the effect of chemotherapy states on OS, we also performed additional multivariate analyses for patients who were not received chemotherapy (n = 78; model C and model D in Table 3). We found that there was no clinical parameter that associated with OS.

Discussion

In the present study, we investigated for the first time the long-term clinical course of patients with indolent ATL with a maximum duration of follow-up of 17.6 years. We found that the prognosis of indolent ATL was poor with the MST of 4.1 years, and the estimated 15-year OS rates were 14.1% with no plateau in the survival curve. The prognosis observed in the present study was poorer than expected. Our results confirmed a recent long-term Brazilian study,[6] that showed a poor OS of less than 20% for indolent ATL. In the present study, we showed that 65.1% of patients died of acute ATL with a median time to transformation of 18.8 months. This finding suggests that most patients with indolent ATL will eventually die of aggressive ATL during their long-term course of illness. These findings suggest that even patients with indolent ATL should be carefully observed by frequent clinical visits.

The cause of death in patients with indolent ATL has not been well reported so far. In the present study, patients with indolent ATL died of various causes such as malignancies other than ATL,

chronic pulmonary diseases, opportunistic infections, and autoimmune diseases, in addition to death from acute ATL after transformation. A previous long-term study, which followed-up 50 HTLV-1 carriers with monoclonal proliferation of T lymphocytes (pre-ATL) for 20 years, also reported that 10 patients died of opportunistic infections such as *Pneumocystis* pneumonia or malignancies other than ATL (skin carcinoma, lung cancer, etc).[16] Patients with indolent ATL were also comorbid with a variety of diseases at diagnosis such as chronic pulmonary disease, opportunistic infections, multiple cancers, and autoimmune diseases in the present study. The pathogens responsible for the opportunistic infections were similar to those observed in patients with AIDS associated with HIV. Opportunistic infection was previously reported as a frequent complication in patients with aggressive or with indolent ATL.[2] These findings suggest that helper T-cell function in indolent ATL might be impaired similar to that in AIDS.[17]

We also presented that chronic pulmonary disease, multiple cancers, and autoimmune diseases were frequent as complications at diagnosis in indolent ATL. The reason why indolent ATL had such immune dysregulation remains unknown. It was recently noted that the origin of the ATL cells in a fraction of the patients was from regulatory T cells expressing FoxP3 and CCR4.[18,19] In the present study, 6 patients also had autoimmune diseases. Among them, 3 patients were treated with immunosuppressive drugs, and of those only one patient with smoldering ATL transformed to acute ATL. Therefore, we were not able to evaluate the effect of comorbid autoimmune diseases and immunosuppressive drug therapy on the risk of transformation or poor prognosis so far. Further studies are warranted to elucidate the mechanisms responsible for the development of hyperimmunity or hypoimmunity in patients with indolent ATL.

Although comparison on OS by subtype is not a primary purpose of this study, it was unexpected that survival rates of smoldering ATL (15-year OS, 12.7%) tended to be lower than chronic ATL (15-year OS, 14.7%), and the MST of smoldering ATL (2.9 years) tended to be shorter than chronic ATL (5.3 years; Table 2; Figure 1B). Transformation rates of smoldering ATL and chronic ATL were 60% (n = 15) and 44% (n = 29), respectively (data not shown), which was also unexpected. Although there was no statistically difference in OS, MST, and transformation rate between the 2 groups, our results were different from a previous short-time follow-up study reported by Shimoyama et al[2] (the 4-year survival rates for smoldering type was 62.8%). It was unknown why the rate of smoldering type was poorer than chronic type in the present study. Some previous studies suggested that skin involvements might be a risk factor for poor prognosis of smoldering ATL.[6,20-22] In the present study, the frequency of patients with skin lesion was a little higher in smoldering ATL (n = 14; 56%) than in chronic ATL (n = 32; 49%). The OS of smoldering ATL with skin lesion was worse than that of chronic ATL without skin lesion (supplemental Figure 2), although there was no statistical difference ($P = .5$). Therefore, a possible explanation might be that smoldering ATL with poor conditions (eg, skin involvement) might be disproportionately included in the present study because data were collected at a university hospital, where more advanced cases were referred from city clinics. Another possible explanation might be that the percentage of patients with smoldering-type ATL has increased recently, as shown in Table 1. In recent decades, more patients have been diagnosed with the smoldering type of ATL on the basis of a health examination, including a blood cell count. Some of these patients may have been in the early phase of acute ATL.

Shimoyama et al[2] reported that involved lymph node lesions, extranodal lesions, and total involvement lesions were significantly poor prognostic factors for ATL all together, and low serum albumin, high LDH, or high BUN levels were PPFs for chronic ATL.[13,14] As we expected, patients with at least 1 of 3 known PPFs for chronic ATL (a high level of LDH and BUN and a low level of albumin)[13,14] showed a poor survival rate than patients without (Table 2; Figure 2D). We also confirmed the difference was seen when analyses were performed for chronic ATL only ($P = .03$) but was not seen for smoldering ATL only ($P = .62$; supplemental Figure 3). This suggests that there may be different prognostic factors for smoldering ATL and chronic ATL, respectively. Further detailed studies regarding prognostic factors are needed for individual subtype.

Other than the known 3 potential prognostic factors, an advanced PS, neutrophilia, more than 3 extranodal lesions, more than 4 total involved lesions, and having received chemotherapy were shown to be possible unfavorable prognostic factors for indolent ATL in our Kaplan-Meier analyses (Table 2; Figures 1B, 2A-F). However, in multivariate Cox analyses, only advanced PS and chemotherapy state were associated with OS after adjustment for other covariates (models A and B in Table 3). The poor prognosis in patients with indolent ATL who were treated by chemotherapy was similar to that of the patients with unfavorable chronic ATL who were treated with intensive combination chemotherapy in several clinical trials in Japan.[3,5,23] Although advanced PS was a borderline significant independent poor factor on survival for indolent ATL in the model that used all patients, the factor was not a prognostic factor anymore when data were limited for only untreated patients (models C and D in Table 3). Among 12 patients who received chemotherapy, 7 (58%) had advanced PS at diagnosis. This suggests that patients with advanced PS at diagnosis might have a condition that required treatments, which introduced the disappearance of the effect of advanced PS on survival, even though advanced PS was an independent poor factor.

Regarding the effect of the presence of extranodal lesions on poor survival, we previously reported that BM involvement was a prognostic factor for aggressive ATL.[24] Although we did not present the effect of each extranodal lesion on survival in detail, we also confirmed that the survival rate of patients with BM involvement was significantly poor compared with patients those without BM involvement ($P = .04$; data not shown), but the survival rate of patients with skin involvement was not different compared with those without ($P = .66$; supplemental Figure 2). However, some studies reported that the presence of skin lesions was a possible poor prognostic factor in indolent ATL,[6,20-22] as described earlier. Setoyama et al[21] reported that smoldering cases with a deeper infiltration pattern had a more aggressive course than cases with a superficial infiltration pattern. Degree of skin involvement might be associated with prognosis in indolent ATL.

Previously, our study group noted that some patients showed alterations in tumor suppressor genes (p16 INKA[25,26] or p53[27]) or aneuploidy greater than 1 chromosomal locus by comparative genomic hybridization in ATL cells[28] and that such abnormalities were associated with a poor prognosis. Although we could not perform molecular analyses for all patients in the present study, 7 were examined molecularly, and at least one abnormality was found in each patient (data not shown). They had a poor prognosis and died within 2.5 years. Patients with a poor prognosis who died during the first steep slope in the survival curve (Figure 1A) might have had such genetic alterations.

The primary purpose of this study was to analyze prognosis of smoldering and chronic types together as an indolent type of ATL. Therefore, we were not able to present in detail the difference in

prognostic factors between subtypes, which is one of the limitations in this study. The number of cases evaluated in this study was too small to perform detail analyses for prognostic factors in indolent ATL. Further large-scaled studies are warranted.

In conclusion, the long-term prognosis of patients with indolent ATL was not good without a plateau phase in the survival curve. Further studies are warranted to elucidate patients with indolent ATL who require intensive chemotherapy, allogenic hematopoietic stem cell transplantation (in cases of aggressive ATL), or combination therapy with zidovudine and interferon alfa.[29,30] In addition, new molecular targeting treatments, such as histone deacetylase inhibitors,[31] which have shown promise in the treatment of $CD4^+$ cutaneous T-cell lymphoma, should be taken into consideration for treatment of indolent ATL.

Acknowledgments

We thank the many hematologists in the Department of Hematology and Molecular Medicine, Atomic Bomb Disease Institute, Nagasaki University, Graduate School of Biomedical Sciences, for the diagnosis and treatment of patients with ATL.

No grants or financial support were provided for this study.

Authorship

Contribution: Y.T. collected and analyzed the data and wrote the manuscript; M.I. analyzed the data and wrote the manuscript; Y.I., M.T., T.J., T.K., Y.Y., S.K., S.I., Y.M., and M.T. made the diagnoses and treated the patients with ATL; and K.T. organized the study.

Conflict-of-interest disclosure: The authors declare no competing financial interests.

Correspondence: Masako Iwanaga, Department of Molecular Medicine and Hematology, Atomic Bomb Disease Institute, Nagasaki University Graduate School of Biomedical Sciences, 1-12-4 Sakamoto, Nagasaki 852-8523, Japan; e-mail: masakoiwng@gmail.com.

References

1. IARC Working Group on the Evaluation of Carcinogenic Risks to Humans. Human immunodeficiency viruses and human T-cell lymphotropic viruses. In: *IARC Monographs on the Evaluation of Carcinogenic Risks to Humans*. Vol 67. Lyon, France: IARC; 1996:261-390.
2. Shimoyama M. Diagnostic criteria and classification of clinical subtype of adult T-cell leukemia-lymphoma: a report from the Lymphoma Study Group (1984-87). *Br J Haematol*. 1991;79(3):428-437.
3. Yamada Y, Tomonaga M, Fukuda H, et al. A new G-CSF-supported combination chemotherapy, LSG15, for adult T-cell leukaemia-lymphoma: Japan Clinical Oncology Group Study 9303. *Br J Haematol*. 2001;113(2):375-382.
4. Fukushima T, Miyazaki Y, Honda S, et al. Allogeneic hematopoietic stem cell transplantation provides sustained long-term survival for patients with adult T-cell leukemia/lymphoma. *Leukemia*. 2005;19(5):829-834.
5. Tsukasaki K, Utsunomiya A, Fukuda H, et al. VCAP-AMP-VECP compared with biweekly CHOP for adult T-cell leukemia-lymphoma: Japan clinical oncology group study JCOG 9801. *J Clin Oncol*. 2007;25(34):5458-5464.
6. Bittencourt AL, da Graças Vieira M, Brites CR, Farre L, Barbosa HS. Adult T-cell leukemia/lymphoma in Bahia, Brazil: analysis of prognostic factors in a group of 70 patients. *Am J Clin Pathol*. 2007;128(5):875-882.
7. Yoshida M, Seiki M, Yamaguchi K, et al. Monoclonal integration of human T-cell leukemia provirus in all primary tumors of adult T-cell leukemia suggests causative role of human T-cell leukemia virus in the disease. *Proc Natl Acad Sci U S A*. 1984;81(8):2534-2537.
8. Yamada Y. Phenotypic and functional analysis of leukemic cells from 16 patients with adult T-cell leukemia/lymphoma. *Blood*. 1983;61(1):192-199.
9. Tsukasaki K, Ikeda S, Murata K, et al. Characteristics of chemotherapy-induced clinical remission in long survivors with aggressive adult T-cell leukemia/Lymphoma. *Leuk Res*. 1993;17(2):157-166.
10. Dale DC. Neutropenia and neutrophilia. In: Lichtman MA, Beutler E, Kipps TJ, Seligsohn U, Kaushansky K, Prchal JT, eds. *Williams Hematology*. 7th ed. New York: McGraw Hill; 2006:907-919.
11. Wardlaw A. Eosinophils and their disorders. In: Lichtman MA, Beutler E, Kipps TJ, Seligsohn U, Kaushansky K, Prchal JT, eds. *Williams Hematology*. 7th ed. New York: McGraw Hill; 2006:863-878.
12. Major prognostic factors of patients with adult T-cell leukemia-lymphoma: a cooperative study. Lymphoma Study Group (1984-1987). *Leuk Res*. 1991;15(2-3):81-90.
13. Shimoyama M. Chemotherapy of ATL. In: Takatsuki K, ed. *Adult T-Cell Leukemia*. Oxford, United Kingdom: Oxford University Press; 1994: 221-237.
14. Tobinai K, Watanabe T. Adult T-cell leukemia-lymphoma. In: Abeloff MD, Armitage JO, Niederhuber JE, Niederhuber JE, Kastan MB, McKenna WG, eds. *Clinical Oncology*. 3rd ed. Philadelphia, PA, Elsevier Churchill Livingstone; 2004:3109-3130.
15. Shimoyama M, Ota K, Kikuchi M, et al. Chemotherapy results and prognostic factors of patients with advanced non-Hodgkin's lymphoma treated with VEPA or VEPA-M. *J Clin Oncol*. 1988;6(1): 128-141.
16. Imaizumi Y, Iwanaga M, Tsukasaki K, et al. Natural course of HTLV-1 carriers with monoclonal proliferation of T lymphocytes (pre-ATL) in a 20-year follow-up study. *Blood*. 2005;105(2):903-904.
17. Soumelis V, Scott I, Gheyas F, et al. Depletion of circulating natural type 1 interferon-producing cells in HIV-infected AIDS patients. *Blood*. 2001; 98(4):906-912.
18. Kohno T, Yamada Y, Akamatsu N, et al. Possible origin of adult T-cell leukemia/lymphoma cells from human T lymphotropic virus type-1-infected regulatory T cells. *Cancer Sci*. 2005;96(8):527-533.
19. Matsubar Y, Hori T, Morita R, et al. Delineation of immunoregulatory properties of adult T-cell leukemia cells. *Int J Hematol*. 2006;84(1):63-69.
20. Ishida T, Utsunomiya A, Iida S, et al. Clinical significance of CCR4 expression in adult T-cell leukemia/lymphoma: its close association with skin involvement and unfavorable outcome. *Clin Cancer Res*. 2003;9(10 Pt 1):3625-3634.
21. Setoyama M, Katahira Y, Kanzaki T. Clinicopathologic analysis of 124 cases of adult T-cell leukemia/lymphoma with cutaneous manifestations: the smouldering type with skin manifestations has a poorer prognosis than previously thought. *J Dermatol*. 1999;26(12):785-790.
22. Ishitsuka K, Ikeda S, Utsunomiya A, et al. Smouldering adult T-cell leukaemia/lymphoma: a follow-up study in Kyushu. *Br J Haematol*. 2008; 143(3):442-444.
23. Yamada Y, Tomonaga M. The current status of therapy for adult T-cell leukaemia-lymphoma in Japan. *Leuk Lymphoma*. 2003;44(4):611-618.
24. Takasaki Y, Iwanaga M, Tsukasaki K, et al. Impact of visceral involvements and blood cell count abnormalities on survival in adult T-cell leukemia/lymphoma (ATLL). *Leuk Res*. 2007;31(6):751-757.
25. Yamada Y, Hatta Y, Murata K, et al. Deletion of p15 and/or p16 genes as a poor-prognosis factor in adult T-cell leukemia. *J Clin Oncol*. 1997;15(5): 1778-1785.
26. Takasaki Y, Yamada Y, Sugahara K, et al. Interruption of p16 gene expression in adult T-cell leukaemia/lymphoma: clinical correlation. *Br J Haematol*. 2003;122(2):253-259.
27. Tawara M, Hogerzeil SJ, Yamada Y, et al. Impact of p53 aberration on the progression of adult T-cell leukemia/lymphoma. *Cancer Lett*. 2006;234(2): 249-255.
28. Tsukasaki K, Krebs J, Nagai K, et al. Comparative genomic hybridization analysis in adult T-cell leukemia/lymphoma: correlation with clinical course. *Blood*. 2001;97(2):3875-3881.
29. Termine O, Bouscary D, Gessain A, et al. Brief reports: treatment of adult T-cell leukaemia-lymphoma with zidovudine and interferon alfa. *N Engl J Med*. 1995;332(26):1749-1751.
30. Bazarbachi A, Hermine O. Treatment of adult T-cell leukaemia/lymphoma: current strategy and future perspectives. *Virus Res*. 2001;78(1-2):79-92.
31. Mori N, Matsuda T, Tadano M, et al. Apoptosis induced by the histone deacetylase inhibitor FR901228 in human T-cell leukemia virus type 1-infected T-cell lines and primary adult T-cell leukemia cells. *J Virol*. 2004;78(9):4582-4590.

Oncogene (2010) 29, 4157–4169

www.nature.com/onc

ORIGINAL ARTICLE

Downregulation of ZEB1 and overexpression of Smad7 contribute to resistance to TGF-β1-mediated growth suppression in adult T-cell leukemia/lymphoma

S Nakahata[1], S Yamazaki[2], H Nakauchi[2] and K Morishita[1]

[1]*Division of Tumor and Cellular Biochemistry, Department of Medical Sciences, Faculty of Medicine, University of Miyazaki, Miyazaki, Japan and* [2]*Laboratory of Stem Cell Therapy, Center for Experimental Medicine, The Institute of Medical Science, University of Tokyo, Tokyo, Japan*

Zinc-finger E-box binding homeobox 1 (*ZEB1*) is a candidate tumor-suppressor gene in adult T-cell leukemia/lymphoma (ATLL). *ZEB1* binds phosphorylated Smad2/3 to enhance transforming growth factor-β1 (TGF-β1) signaling. In addition to downregulation of *ZEB1* mRNA, we found overexpression of inhibitory Smad, Smad7, in resistance of ATLL cells to growth suppression by TGF-β1. A protein complex of Smad7 and histone deacetylase constantly bound to the promoter region of TGF-β1 responsive genes with the Smad-responsive element (SRE) to inhibit TGF-β1 signaling; however, ectopic expression of ZEB1 reactivated TGF-β1 signaling by binding to Smad7 and recruiting the Smad3/p300 histone acetyltransferase complex to the promoter after TGF-β1 stimulation in ATLL. Conversely, because *ZEB1* mRNA was detected in the late stages of T-cell development, we used CTLL2 cells with *ZEB1* expression, a murine peripheral T-cell lymphoma, and found that a complex of Smad3, Smad7 and ZEB1 was bound to the SRE of the $p21^{CDKN1A}$ promoter after the induction of Smad7 by TGF-β1 treatment. Because the duration of TGF-β1-induced transcriptional activation of *PAI-1* and *p21* was shortened in shZEB1-expressing CTLL2 cells, ZEB1 may have a role in enhancing TGF-β1 signaling by binding not only to Smad3 but also to Smad7 in the nucleus. Altogether, these results suggest that both ZEB1 downregulation and Smad7 overexpression contribute to resistance to TGF-β1-mediated growth suppression in ATLL.
Oncogene (2010) **29**, 4157–4169; doi:10.1038/onc.2010.172; published online 31 May 2010

Keywords: ZEB1; Smad7; ATLL

Introduction

Adult T-cell leukemia/lymphoma (ATLL) is a malignant and fatal disorder of $CD4^+$ T cells that is caused by infection of these cells with human T-cell leukemia virus type I (HTLV-1). ATLL occurs in 3–5% of HTLV-1 carriers following a long latency period, which can range from 40 to 60 years (Yasunaga and Matsuoka, 2003). ATLL cells are derived from the malignant clonal expansion of an HTLV-1-infected $CD4^+$ T lymphocyte that has accumulated genetic lesions, including the activation of oncogenes or inactivation of tumor-suppressor genes (Tsukasaki *et al.*, 2001). A previous study from our laboratory discovered these genetic lesions by spectral karyotyping with a high-density single-nucleotide polymorphism array and comparative genomic hybridization in ATLL; we found that the T-cell transcription factor (TCF8)/zinc-finger E-box binding homeobox 1 (ZEB1) was a candidate tumor suppressor in ATLL (Hidaka *et al.*, 2008).

Transcription factors from the ZEB family have been characterized as downstream effectors of the transforming growth factor-β (TGF-β) signaling pathway. ZEB1 binds to receptor-regulated Smad2/3 and synergizes with Smad-mediated transcriptional activation (van Grunsven *et al.*, 2001; Postigo, 2003). TGF-β1 belongs to a superfamily of cytokines that regulates a broad range of cellular responses, including cell proliferation, differentiation, adhesion, migration and apoptosis (Kingsley, 1994). Deregulated TGF-β1 signaling has been implicated in various human diseases, including autoimmune diseases, vascular disorders and cancer (Blobe *et al.*, 2000). TGF-β1 has antiproliferative effects in a variety of cell types, and this negative regulation of cellular proliferation by TGF-β1 functions to suppress the growth of tumor cells (Derynck *et al.*, 2001). However, HTLV-1-infected T cells and ATLL cells are resistant to the growth inhibitory action of TGF-β1, even though these cells express high levels of TGF-β1 (Kim *et al.*, 1990). Although Tax, a viral protein, has been reported to render cells resistant to TGF-β1-mediated growth suppression (Mori *et al.*, 2001; Arnulf *et al.*, 2002), Tax expression is not detectable in most ATLL cells. Therefore, it has been suggested that ATLL cells develop different mechanisms of resistance to escape the antiproliferative signal that is mediated by TGF-β1. One such mechanism might be associated with aberrant expression of MEL1S (Yoshida *et al.*, 2004), which was originally isolated as the gene that was transcriptionally activated by t(1;3)(p36;q21) in acute myeloid leukemia

Correspondence: Dr K Morishita, Division of Tumor and Cellular Biochemistry, Department of Medical Sciences, Faculty of Medicine, University of Miyazaki, 5200 Kihara, Kiyotake, Miyazaki 889-1692, Japan.
E-mail: kmorishi@med.miyazaki-u.ac.jp
Received 19 October 2009; revised 3 March 2010; accepted 19 April 2010; published online 31 May 2010

(Mochizuki *et al*., 2000). We previously reported that *ZEB1* expression was downregulated in a majority of ATLL cells (Hidaka *et al*., 2008). Furthermore, *ZEB1*-mutant mice frequently developed $CD4^+$ T-cell lymphomas and/or leukemias, suggesting that *ZEB1* may have a tumor suppressive role in ATLL. In addition, the enforced expression of ZEB1 partially restored the responsiveness of ATLL cells to TGF-β1. Therefore, the downregulation of *ZEB1* expression may be associated with resistance to the growth inhibitory activity of TGF-β1.

In this paper, we report that Smad7, an inhibitory Smad (I-Smad), is overexpressed in HTLV-1-infected T-cell lines and primary leukemia cells from acute-type ATLL patients. Smad7 is immediately induced after TGF-β stimulation and acts as an antagonist of TGF-β signaling, which may regulate the intensity or duration of its signaling cascade (Shi and Massagué, 2003). Although constitutive expression of Smad7 inhibited TGF-β1 growth suppression in ATLL cells, we found that ectopically expressed ZEB1 overcame the Smad7-mediated inhibition of TGF-β1 signaling. Smad7 constitutively bound to the promoter of the TGF-β1 responsive genes with the Smad-responsive element (SRE) to inhibit TGF-β1 signaling. TGF-β1 stimulation, in the presence of ZEB1 overexpression, led to ZEB1 recruitment of the Smad3 complex to the promoter region with Smad7 to reactivate TGF-β1 signaling. Conversely, *ZEB1* mRNA was expressed in $CD4^+CD8^+$, $CD4^+CD8^-$ and $CD4^-CD8^+$ T cells in the late stages of T-cell development, and using CTLL2, a murine T-lymphoma cell line with *ZEB1* expression, we examined the protein complexes associated with the promoter region of the TGF-β1 responsive genes with SRE and time course for gene expression of the TGF-β1 activating genes *Smad6*, *Smad7*, plasminogen activator inhibitor 1 (*PAI-1*) and cyclin-dependent kinase inhibitor 1A (*p21*). We found that a ternary complex of Smad3, Smad7 and ZEB1 on the *p21* promoter with the SRE kept activating *p21* transcription after the induction of Smad7 by TGF-β1. TGF-β1 stimulation of CTLL2 cells expressing a short hairpin to ZEB1 led to a shorter expression time interval of *PAI-1* and *p21* whereas the expression of *Smad6* and *Smad7* remained unchanged. The results suggest that ZEB1 enhances TGF-β1 signaling by binding not only to the Smad3 complex and but also to Smad7 in the nucleus. Thus, ZEB1 may have important roles in the regulation of TGF-β1 signaling, and both ZEB1 downregulation and Smad7 overexpression may be important molecular events that contribute to resistance to TGF-β1 signaling in ATLL.

Results

Upregulated expression of I-Smad7 in ATLL cells

We previously reported that *ZEB1* expression was downregulated and functioned as a possible tumor suppressor in a majority of ATLL cells (Hidaka *et al*., 2008). ZEB1 has been reported to bind Smad3 and enhance TGF-β1 signaling, and the resistance of HTLV-1-infected T cells and ATLL cells to TGF-β1-mediated growth inhibition is one of the most prominent characteristics of ATLL. Because ectopic expression of ZEB1 in ATLL cells partially restored sensitivity to TGF-β1, the mRNA expression of four Smad family members (Smad2, 3, 6 and 7) that function as modulators of TGF-β1 signaling were analyzed using semiquantitative RT–PCR in four HTLV-1-negative T-acute lymphoblastic leukemia (T-ALL) cell lines (MOLT4, MKB1, KAWAI and Jurkat) (referred as HTLV-1 (−)) and seven HTLV-1-positive cell lines (HTLV-1 (+)). These HTLV-1 (+) cell lines included two HTLV-1-infected cell lines (MT2 and Hut102) and five ATLL-derived cell lines (ED, KOB, SO4, KK1 and S1T) (Figure 1a). The MOLT4 cells and all seven HTLV-1 (+) cell lines had high expression of inhibitory *Smad7*, but not of *Smad6* mRNA, whereas the other three HTLV-1 (−) cell lines (MKB-1, KAWAI and Jurkat) did not express *Smad7* but expressed *Smad6*. In addition, there were no significant differences in the pattern of *Smad2* and *Smad3* expression between the HTLV-1 (−) and HTLV-1 (+) cell lines. Because *HTLV-1 tax/rex* mRNA was expressed in two HTLV-1-infected cell lines (MT2 and Hut102) and two ATLL-derived cell lines (KOB and SO4), the expression patterns of *HTLV-1 tax/rex* did not appear to correlate with the expression of the four members of the Smad family. To confirm that protein levels of ZEB1, Smad3 and Smad7 correlate with the mRNA level in the leukemia cell lines, we analyzed protein expression by western blot (Supplementary Figure 1). In HTLV-1 (+) cells, we detected a significantly higher and lower expression level of Smad7 and ZEB1 mRNA and protein, respectively, compared to HTLV-1 (−) cells.

Next, we used real-time RT–PCR analysis to determine the quantitative expression levels of *Smad7* and *ZEB1* in the same 11 cell lines. The expression of *Smad7* mRNA in the HTLV-1 (+) cell lines and the MOLT4 cell line was significantly higher ($P<0.05$) than in the HTLV-1 (−) cell lines. However, the expression of *ZEB1* mRNA was significantly reduced in the HTLV-1 (+) cell lines (Figure 1b). The *Smad7*/*ZEB1* expression ratio was 10-fold greater in the HTLV-1 (+) cell lines and the MOLT4 cell line compared to the $CD4^+$ T lymphocytes from normal volunteers. To confirm the expression pattern of high Smad7 with low ZEB1 in ATLL cells from patient samples, we used real-time RT–PCR using RNA isolated from ATLL cells derived from eight acute-type ATLL patients and normal $CD4^+$ T lymphocytes. As observed with the cell lines, all ATLL cells from patients with acute-type ATLL had higher Smad7/ZEB1 ratios than the $CD4^+$ T lymphocytes from normal volunteers ($P<0.05$) (Figure 1c). In two patients (no. 4 and 7), the expression of Smad7 was almost equal to the level in normal $CD4^+$ T cells; however, the expression of ZEB1 was clearly decreased, suggesting that the reduction of ZEB1 may contribute to a part of the resistance to TGF-β1 signaling. Alternatively, *Smad6* was weakly expressed in one out of eight ATLL cells and was not expressed in the $CD4^+$ T lymphocytes from normal volunteers (Supplementary Figure 2). Therefore, these data suggest that the higher expression

of I-Smad7 and downregulation of ZEB1 in ATLL cells could potentially modulate the responsiveness to TGF-β1-mediated growth suppression in ATLL cells.

Constitutive expression of Smad7 in ATLL cells renders cells resistant to TGF-β1-mediated growth inhibition

To assess whether the expression levels of ZEB1 and Smad7 could modulate TGF-β1 growth suppression in T-lymphoid cell lines, we downregulated endogenous *Smad7* and *ZEB1* expression in the MOLT4 cell line by transfecting an shRNA expression vector pSIREN-RetroQ-ZsGreen (Clontech, Mountain View, CA, USA) for Smad7 (shSmad7) and/or ZEB1 (shZEB1), as well as one for firefly luciferase, which served as a control (shLuc). Downregulation of *Smad7* and/or *ZEB1* expression was confirmed by semiquantitative (left, Figure 2a) and quantitative RT–PCR (Figure 2b). Approximately 70% of the parental and MOLT4-shLuc cells survived treatment with 10 ng/ml TGF-β1 for 48 h, the maximal inhibitory concentration (right, Figure 2a). In response to treatment with 10 ng/ml TGF-β1, 37% of the MOLT4-shSmad7 and 87% of the MOLT4-shZEB1 cells survived. Approximately 52% of shSmad7/shZEB1-transfected MOLT4 (MOLT4-shZEB1 + shSmad7) survived the TGF-β1 treatment, placing the survival rate of this cell line between the parental-MOLT4-shLuc and MOLT4-shSmad7 cells. We plotted the expression ratio of Smad7 and ZEB1 against the percentages of cell survival after the TGF-β1 treatment in the context of the various transfection conditions for the MOLT4 cell lines. As shown in Figure 2b, the survival rates of TGF-β1 treated MOLT4 cells, with the exception of MOLT4-shZEB1, correlated significantly with the expression ratios of Smad7 and ZEB1 ($R^2 = 0.9682$). Almost all of the HTLV-1 (+) cell lines with significantly high-expression ratios had a similar survival rate of nearly 100% ($R^2 = 0.7333$), suggesting that cell lines with an expression ratio of Smad7/ZEB1 of more than 20-fold have a nearly 100% survival rate after TGF-β1 treatment.

To confirm whether the elevated Smad7 expression had a role in the resistance to TGF-β1 growth inhibition of HTLV-1 (+) cell lines irrespective of Tax expression, we downregulated endogenous Smad7 in Tax-positive MT2 and Tax-negative KK1 cell lines by transfection of a vector expressing shSmad7. The growth of the shSmad7-transfected MT2 and KK1 cells was inhibited by TGF-β1 treatment for 48 h in a dose-dependent manner, whereas both of the parental cells and the control shLuc-transfected cells were completely resistant to the growth inhibitory action of TGF-β1 (Figures 2c and d). In both the Tax-positive cell lines (MT2 and Hut102; Supplementary Figure 3) and the Tax-negative cell lines (MOLT4 and KK1), shSmad7 transfection

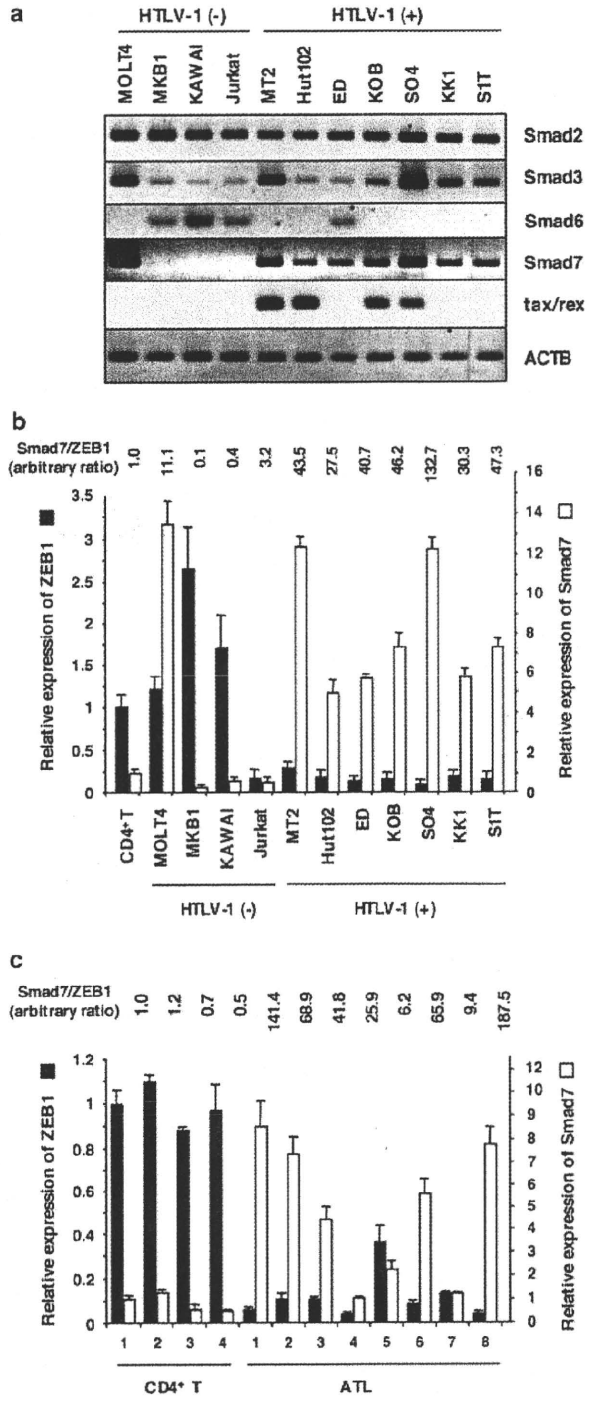

Figure 1 The mRNA expression profile of the Smad family. (**a**) Semiquantitative RT–PCR analysis for *Smad2*, *Smad3*, *Smad6*, *Smad7* and *HTLV-1 tax/rex* is shown in four HTLV-1-negative (MOLT4, MKB1, KAWAI and Jurkat) and seven HTLV-1-positive (MT2, Hut102, ED, KOB, SO4, KK1 and S1T) cell lines. The expression of β-actin (*ACTB*) is shown at the bottom as a control. (**b**) Quantitative RT–PCR analysis for *Smad7* and *ZEB1* is shown in the four HTLV-1-negative and seven HTLV-1-positive cell lines. *Smad7* and *ZEB1* mRNA expression levels were normalized to β-actin mRNA expression and expressed relative to the mRNA level in a healthy control (CD4+T). The relative levels of *Smad7* and *ZEB1* expression are presented as a ratio of *Smad7*/*ZEB1* mRNA. Student's *t*-test was used for the statistical analysis. (**c**) Quantitative RT–PCR analysis for *Smad7* and *ZEB1* is shown in eight patients with acute-type ATLL (ATL) and in four healthy controls (CD4+T). *Smad7* and *ZEB1* mRNA expression levels were expressed relative to the mRNA level in a healthy control. The data are presented as in Figure 1b.

enhanced the growth-suppression effect of TGF-β1. In addition, enforced expression of ZEB1 in many HTLV-1 (+) cell lines enhanced TGF-β1 growth suppression, suggesting that Tax expression was independent of the modulation of TGF-β1 responsiveness by *Smad7* and *ZEB1* expression.

ZEB1 counteracts Smad7 repression of TGF-β1 signal transduction

To determine how the expression of Smad6, Smad7 and/or ZEB1 is involved in TGF-β1 signaling, we assayed the activity of the promoter in HepG2 hepatocellular carcinoma cells using a luciferase reporter plasmid with the TGF-β1-responsive elements from the *PAI-1* promoter (p3TP-Lux). Co-transfection of Smad6 with the 3TP-Lux promoter vector weakly inhibited the TGF-β1-induced transcriptional activity, and co-transfection of Smad7 significantly inhibited TGF-β1-induced transcription (Figure 3a). Co-transfection of ZEB1 alone enhanced the TGF-β1-induced 3TP-Lux promoter activity (Figure 3b), probably through a direct interaction with Smad3 (Postigo, 2003). Importantly, co-transfection of ZEB1 with Smad6 or Smad7 overcame the inhibition of TGF-β1 signaling in a dose-dependent manner (Figure 3b). These results suggest that ZEB1 might counteract the Smad6- and Smad7-mediated inhibition of TGF-β1 growth suppression.

To determine the physical interaction between ZEB1 and I-Smad proteins, we performed co-immunoprecipitation experiments using 293T cells that were transiently transfected with ZEB1 and FLAG-tagged Smad6 or Smad7 expression plasmids. As shown in Figure 3c, ZEB1 coprecipitated with Smad6 or Smad7, indicating that ZEB1 could interact with both of the I-Smad proteins. To assess whether ZEB1 could directly modulate the Smad7-mediated inhibition of TGF-β1 signaling in ATLL cells, we evaluated the protein interaction and subcellular localization of endogenous ZEB1 and Smad7 proteins. To detect the physical interaction of endogenous ZEB1 with Smad7 or Smad3, we immunoprecipitated whole-cell lysates from MOLT4 cells treated with or without TGF-β1 for 24 h with an anti-ZEB1 antibody, and the immune complexes were

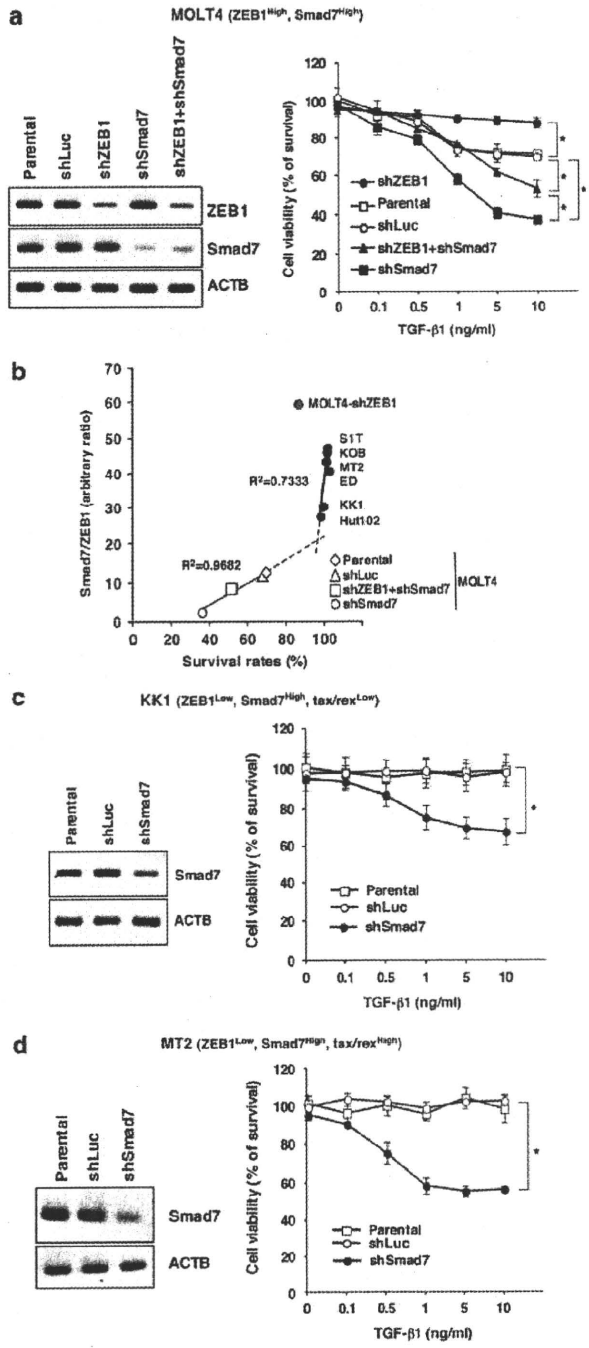

Figure 2 Correlation between expression levels of Smad7 and ZEB1 and responsiveness to TGF-β1. (**a**) Effect of downregulation of endogenous Smad7 and ZEB1 on TGF-β1-induced growth inhibition in MOLT4 cells. (Left) Semiquantitative RT–PCR analysis was performed with mRNA isolated from MOLT4 cells that were either untransfected (Parental) or transfected with the control luciferase-specific shRNA (shLuc), the Smad7-specific shRNA (shSmad7), the ZEB1-specific shRNA (shZEB1) or both the ZEB1- and Smad7-specific shRNA vectors (shZEB1 + shSmad7). PCR for *Smad7*, *ZEB1* and β-actin are shown. (Right) Viable cells after treatment with the indicated concentration of TGF-β1 for 48 h were examined using the MTT assay and are shown as the percentages of the values obtained from the unstimulated parental cells. The cell number per ml at time zero was 4×10^4. Student's *t*-test was used for the statistical analysis, and $P<0.05$ (asterisk) was considered significant. (**b**) Correlation between the expression ratios of *Smad7* and *ZEB1* and cell survival rates after TGF-β1 treatment in various transfected MOLT4 cells versus various HTLV-1 (+) cell lines. Scatter plots with a smooth trend line are shown. The coefficient of correlation (R^2) is indicated for each trend line. (**c**, **d**) The effect of downregulation of endogenous Smad7 in TGF-β1-induced growth inhibition in Tax-non-expressing (**c**) and Tax-expressing (**d**) HTLV-1-positive cell lines. Semiquantitative RT–PCR analysis and viable cell counts were performed with KK1 and MT2 cells that were untransfected (Parental) or transfected with either the control luciferase-specific shRNA vector (shLuc) or the Smad7-specific shRNA vector (shSmad7). (Left) Semiquantitative RT–PCR for *Smad7* and β-actin mRNA are shown in each cell line. (Right) After transfection with the shRNA vectors, the cells were treated with the indicated concentration of TGF-β1 for 48 h. The degree of proliferation of each cell line was examined by MTT assay. The data are presented as in Figure 2a.

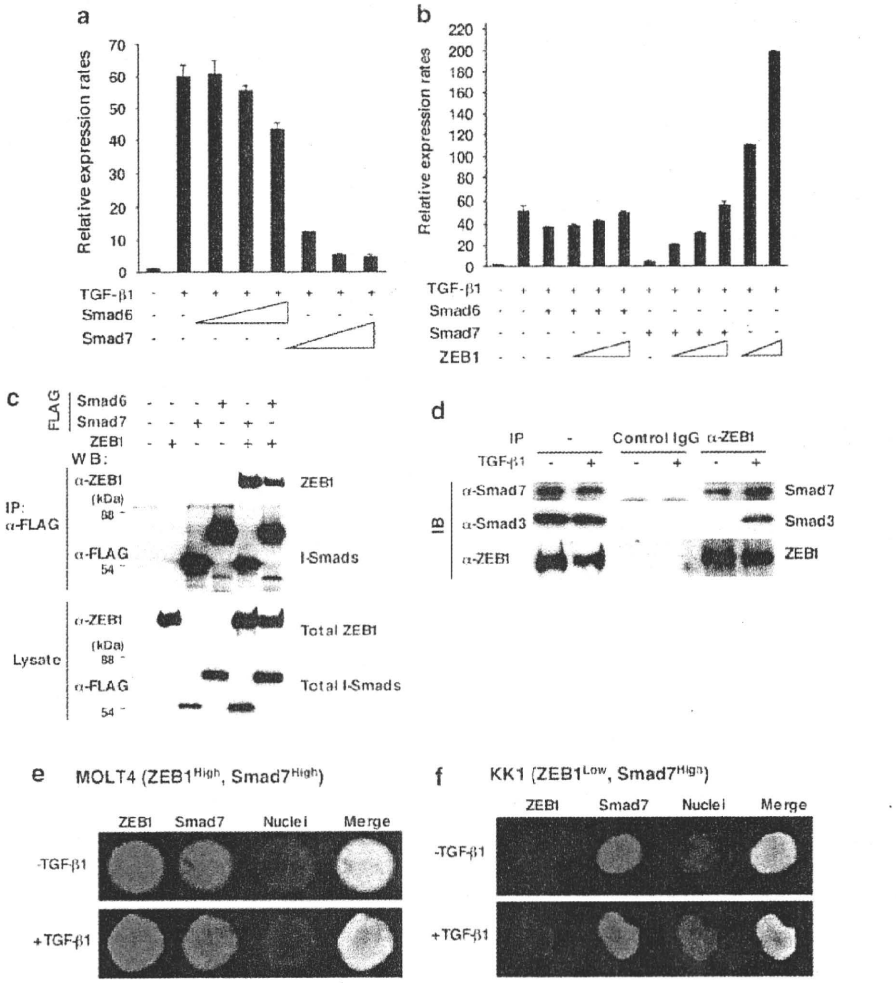

Figure 3 Counteraction of TGF-β1 signal transduction by ZEB1 and Smad7. (**a**) Smad7 expression significantly decreases the TGF-β1 responsiveness of a Smad-dependent gene promoter. 3TP-Lux reporter assays were performed in HepG2 cells with co-transfection of either control pcDNA3 (−), increasing amounts of FLAG-Smad7/pcDNA3 or FLAG-Smad6/pcDNA3, and 3TP-Lux reporter plasmid plus stimulation by 5 ng/ml of TGF-β1 (+) or phosphate-buffered saline (PBS) (−) for 24 h. The results are shown as the means and s.d. of triplicate transfections. The activity obtained in the absence of TGF-β1 was set at 1. (**b**) ZEB1 counteracts the inhibitory effects of Smad6 or Smad7. 3TP-Lux reporter assays were performed in HepG2 cells transiently transfected with pcDNA3 (−), FLAG-Smad6/pcDNA3 or FLAG-Smad7/pcDNA3, and/or increasing amounts of the ZEB1/pcDNA and 3TP-Lux reporter plasmids. Cells were stimulated with 5 ng/ml of TGF-β1 (+) or PBS (−) for 24 h. (**c**) ZEB1 interacts with Smad6 or Smad7. 293T cells were transiently transfected with ZEB1, FLAG-Smad7 and/or FLAG-Smad6 expression plasmids, and the whole-cell lysates were immunoprecipitated with an anti-FLAG antibody. The immunoprecipitates were detected by anti-ZEB1 or anti-FLAG antibody. (**d**) Endogenous ZEB1 interacts with endogenous Smad7 or Smad3 in MOLT4 cells. After treatment with 10 ng/ml of TGF-β1 or PBS as control for 24 h, whole-cell lysates from MOLT4 cells were immunoprecipitated with an anti-ZEB1 antibody. The immunoprecipitates were immunoblotted using anti-Smad7 or anti-Smad3 antibody. (**e**, **f**) Subcellular localization of ZEB1 and Smad7 in the absence or presence of TGF-β1 stimulation. After MOLT4 (**e**) and KK1 (**f**) cells were treated with 10 ng/ml of TGF-β1 (+TGF-β1) or PBS (−TGF-β1) for 24 h, localization of endogenous ZEB1 and Smad7 was detected by indirect immunofluorescence using anti-ZEB1 and anti-Smad7 antibodies. The proteins were visualized using an Alexa Fluor 488-conjugated anti-goat secondary antibody (green, for ZEB1) and the Alexa Fluor 555-conjugated anti-rabbit secondary antibody (red, for Smad7). The cells were analyzed using confocal microscopy, and the DAPI (4,6-diamidino-2-phenylindole) stain was used to visualize the nuclei.

subjected to immunoblot analysis using an anti-Smad3 or anti-Smad7 antibody (Figure 3d). The binding of ZEB1 to Smad3 was only detected in the presence of TGF-β1; however, Smad7 consistently co-precipitated with ZEB1 in both the absence and presence of TGF-β1.

Next, to confirm the interaction and subcellular localization of endogenous ZEB1 and Smad7 proteins, both proteins in MOLT4-TALL and KK1-HTLV1 (+) cell lines were immunostained with different fluorescent dyes with either anti-ZEB1 or anti-Smad7 antibody, and the labeled proteins were examined using a confocal microscope. The specificity of the antibody against Smad7 was evaluated by shRNA knockdown experiments. Smad7 was significantly reduced in the shSmad7-

treated cells but not in the shLuc-transfected cells by immunoblots and immunofluorescent staining (Supplementary Figure 4). In MOLT4 cells, ZEB1 and Smad7 were mainly colocalized in the nucleus (Figure 3e), confirming the protein interaction between endogenous ZEB1 and Smad7 (Figure 3d). Nuclear localization of Smad7 was also observed in the KK1-HTLV1 (+) cell line (Figure 3f). Therefore, ZEB1 may directly modulate the inhibitory function of Smad7 in the nucleus.

Association of ZEB1 with Smad7 or Smad3

To investigate the function of ZEB1 in the TGF-β1 signaling pathway, we initially examined the physical interactions between ZEB1, Smad3 and Smad7 with or without TGF-β1 treatment in HepG2 cells using immunoprecipitation and western blot. This was done because both the exogenously expressed ZEB1 and Smad7 were located in the nucleus regardless of TGF-β1 treatment (Supplementary Figure 5). In the absence of TGF-β1 treatment, neither the Smad3–ZEB1 nor Smad3–Smad7 interaction was observed by the coprecipitation assay using the corresponding specific antibody. After TGF-β1 treatment, Smad3 could be precipitated with ZEB1, but not with Smad7 (Supplementary Figure 6a). By contrast, Smad7 was constitutively associated with ZEB1 in HepG2 cells irrespective of TGF-β1 treatment (Supplementary Figure 6b). To identify the binding domain in Smad7 that was responsible for the interaction with ZEB1, we generated two Flag-tagged deletion mutants of Smad7: Smad7-N, which encoded the first half of Smad7 (amino acids 1–259), and Smad7-MH2, which encoded the second half of Smad7 containing the Mad-homology 2 (MH2) domain (amino acids 260–420) (Figure 4a). As shown in Figure 4b, ZEB1 did not coprecipitate with Smad7-N; however, ZEB1 did coprecipitate with Smad7-MH2. This suggests that ZEB1 interacts with the MH2 domain of Smad7. The Smad-interacting domain (SID) of ZEB1 has been reported to interact with Smad1, Smad2 or Smad3 in the nucleus after treatment with TGF-β1 (Postigo, 2003). Therefore, to determine which region of ZEB1 was necessary for binding to Smad7, three deletion mutant plasmids and a full-length *ZEB1* expression plasmid were generated (Figure 4a): a full-length ZEB1–GFP fusion construct (GFP-ZEB1), GFP fused to the N-terminal domain (amino acids 1–377; ZEB1-N), GFP fused to the SID (amino acids 378–457; ZEB1-SID) and GFP fused to the C-terminal domain (amino acids 458–1125; ZEB1-C). As shown in Figure 4c, only ZEB1-SID precipitated with Smad7 protein, suggesting that Smad7 interacts with the SID domain of ZEB1.

Because the SID region of ZEB1 interacts with both Smad3 and Smad7, it is possible that these two proteins compete for ZEB1 in the nucleus after TGF-β1 stimulation. To test this possibility, we transfected HepG2 cells with expression plasmids encoding three genes (*HA-Smad3*, *GFP-Smad7* and *FLAG-ZEB1*) in various combinations and treated with TGF-β1. As shown in Figure 4d, the ZEB1/Smad3, ZEB1/Smad7 and ZEB1/Smad3/Smad7 complexes could all be detected. The same interaction experiment was repeated with the difference being that the full-length *ZEB1* expression plasmid was replaced with a plasmid expressing solely the SID region of ZEB1 (GFP-ZEB1-SID). As shown in Supplementary Figure 7, the ZEB1-SID coprecipitated with Smad3, Smad7 and a complex of Smad3 and Smad7. Because Smad3 and Smad7 have not been shown to interact with each other, these data suggest that the SID region of ZEB1 may simultaneously interact with both Smad3 and Smad7. To assess this possibility, we immunoprecipitated lysates from cells transfected with HA-Smad3, FLAG-Smad7 and ZEB1 in the presence of TGF-β1 with either anti-HA or anti-FLAG antibody and coprecipitation of these three proteins was examined. As shown in Figure 4e, the ZEB1/Smad3/Smad7 complexes were identified in both anti-HA (Smad3) and anti-FLAG (Smad7) immunoprecipitates. We also performed a competitive binding experiment using cells that were co-transfected with a fixed amount of ZEB1-SID and Smad3 expression plasmids and increasing amounts of Smad7 expression plasmid (Figure 4f). After immunoprecipitation of GFP-ZEB1-SID, the ZEB1/SID/Smad3 complex could be detected regardless of the amount of Smad7 expression plasmid that was transfected into the cell. In the converse experiment, ZEB1/SID/Smad7 complex could be detected regardless of the amount of Smad3 expression plasmid that was transfected into the cells (Supplementary Figure 8). Therefore, regulatory Smad3 (R-Smad3) and I-Smad7 were able to bind to the ZEB1-SID region without competition.

Binding of the 3TP promoter region by a transcription factor complex of Smad3, Smad7 and ZEB1 after TGF-β1 stimulation

To investigate the transcriptional regulation by ZEB1 and the Smad proteins, we performed chromatin immunoprecipitation (ChIP) in HepG2 cells co-transfected with the p3TP-Lux and expression plasmids encoding HA-Smad3, FLAG-Smad7 and/or ZEB1. Formaldehyde crosslinked DNA isolated from transfected HepG2 cells was immunoprecipitated using the indicated antibody and subjected to semiquantitative PCR with primers specific for the 3TP promoter. After the transfection of HepG2 cells with the HA-Smad3 expression plasmid, we treated the cells with TGF-β1, and precipitated DNA fragments that bound to the protein complex with either an anti-HA (Smad3), anti-p300 or anti-HDAC1 antibody. Treatment with TGF-β1 induced a dramatic increase in the binding of the 3TP promoter region by both Smad3 and p300 (Figure 5a). Upon transfection of FLAG-Smad7 in either the absence or presence of TGF-β1, the Smad7 and HDAC1 complex was constantly bound to the 3TP promoter (Figure 5b). In addition, when HA-Smad3 and FLAG-Smad7 were co-transfected in the presence of TGF-β1 (Figure 5c), the Smad7/HDAC1 complex was found bound to the 3TP promoter; however, binding of the Smad3 and p300 complex to the promoter was

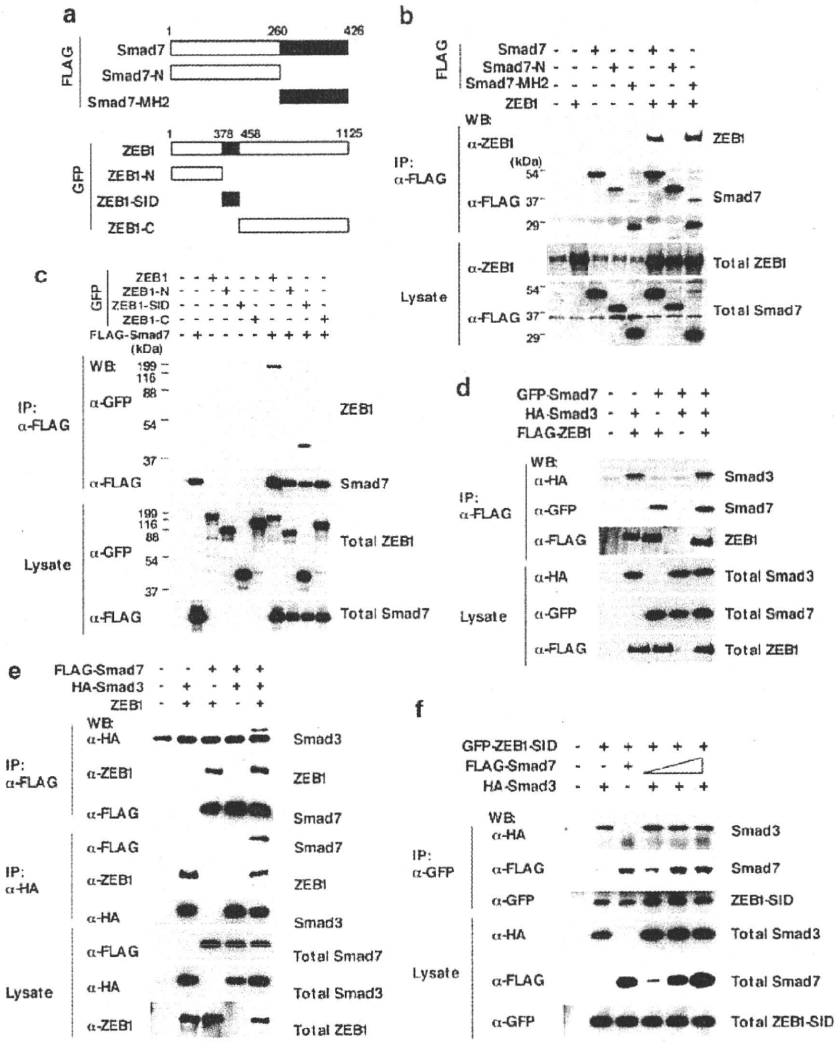

Figure 4 Mapping of the binding site involved in ZEB1/Smad complex formation. (**a**) Schematic representation of Smad7 and ZEB1. White bar indicates the C-terminal deletion mutant lacking the MH2 (Mad-homology 2) domain in Smad7 (Smad7-N). Black bar indicates the N-terminal deletion mutant of Smad7 (SMad7-MH2). The ZEB1-N mutant has 1–377 amino-acid residues before the Smad-interacting domain (SID), ZEB1-SID has the SID (378–457 aa), and the ZEB1-C mutant has the C-terminal region from SID (458–1125 aa). The numbers indicate the amino-acid residue. (**b**) The MH2 domain in Smad7 interacts with ZEB1. After transfection with expression vectors encoding FLAG-Smad7, FLAG-Smad7-N, FLAG-Smad7-MH2 and/or ZEB1 into 293T cells, cell lysates were immunoprecipitated with anti-FLAG antibody. The precipitates were immunoblotted with anti-ZEB1 or anti-FLAG antibody. (**c**) The SID domain in ZEB1 interacts with Smad7. After transfection with an expression vector encoding FLAG-Smad7 and/or various GFP-tagged ZEB1 constructs (Figure 4a) in 293T cells, the cell lysates were immunoprecipitated with anti-FLAG antibody. (**d**) ZEB1 interacts with Smad3 and Smad7. After transfection with FLAG-ZEB1, GFP-Smad7 and HA-Smad3 into HepG2 cells, the cells were treated with 5 ng/ml of TGF-β1 for 24 h. Cell lysates were precipitated by anti-FLAG antibody. The precipitates were immunoblotted by an anti-HA, anti-GFP or anti-FLAG antibody. (**e**) ZEB1 simultaneously interacts with both Smad3 and Smad7. After transfection with ZEB1, FLAG-Smad7, and HA-Smad3 into HepG2 cells, the cells were treated with 5 ng/ml of TGF-β1 for 24 h. Cell lysates were precipitated by either anti-FLAG or anti-HA antibody. The precipitates were immunoblotted by an anti-HA, anti-FLAG or anti-ZEB1 antibody. (**f**) Smad3 and Smad7 interact with ZEB1 in a noncompetitive manner. After transfection with GFP-ZEB1-SID, FLAG-Smad3 and/or increasing amounts of FLAG-Smad7 into HepG2 cells, the cells were treated with 5 ng/ml of TGF-β1 for 24 h and the cell lysates were immunoprecipitated with an anti-GFP antibody.

decreased. When cells were co-transfected with ZEB1, Smad3 and Smad7 in the presence of TGF-β1 (Figure 5d), the binding of Smad3 and p300 was clearly increased to similar levels as that seen with Smad3 transfection alone, while the occupancy of HDAC1 was decreased. The recruitment of ZEB1 to the 3TP promoter region is mediated by its interaction with Smad3 or Smad7, because no signal was detected when the cells were transfected with ZEB1 alone (Supplementary Figure 9). To examine whether *ZEB1* expression in HTLV-I (+) cell lines results in the binding of the Smad7/ZEB1/Smad3/p300 complex to the 3TP promoter region following TGF-β1 stimulation, we performed ChIP in MT2 cells that were co-transfected with the

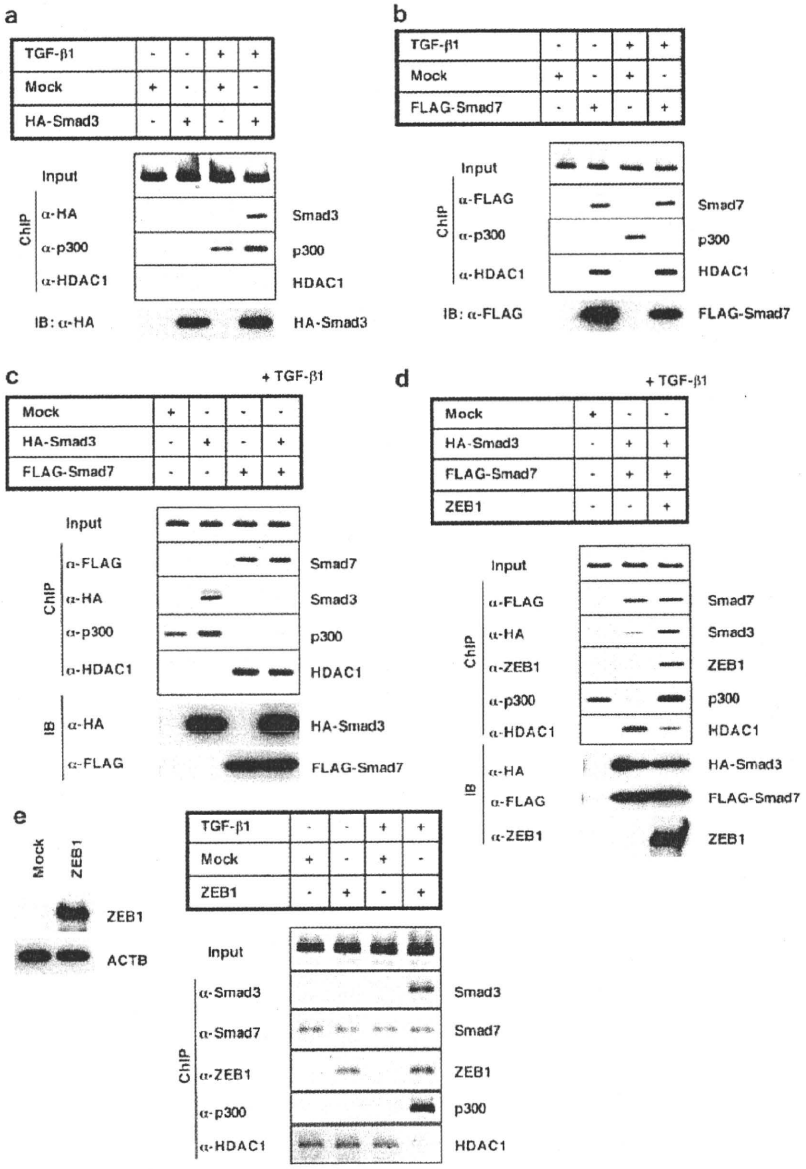

Figure 5 Smad7, ZEB1 and Smad3 are present in the transcription factor complex that binds to the Smad-responsive promoter. (**a**) Specific binding of Smad3 to the 3TP-Lux promoter upon TGF-β1 stimulation. After transfection with pcDNA3 (Mock) or HA-Smad3 and p3TP-Lux into HepG2 cells, the cells were treated with 5 ng/ml of TGF-β1 (+TGF-β1) or phosphate-buffered saline (PBS) (−TGF-β1) for 16 h. The cells were fixed with formaldehyde, sonicated and the chromatin fraction was immunoprecipitated using anti-HA, anti-p300 or anti-HDAC1 antibody. The precipitated DNA and 1% of the input cell lysates were amplified by PCR using specific primers for the 3TP-Lux promoter. As a control, the expression level of HA-tagged Smad3 protein was confirmed by western blot using an anti-HA antibody (IB). (**b**) Smad7 constantly binds to the 3TP-Lux promoter in either the presence or absence of TGF-β1. After transfection with pcDNA3 (Mock) or FLAG-Smad7 with p3TP-Lux and treatment with 5 ng/ml of TGF-β1 (+TGF-β1) or PBS (−TGF-β1) for 16 h, the HepG2 cells were chromatin immunoprecipitated (ChIP) by each indicated antibody. The precipitated DNAs were amplified by the 3TP promoter-specific primers. Smad7 protein expression was identified by an anti-FLAG antibody (IB). (**c**) Smad7 inhibits the DNA-binding of Smad3 and p300. HepG2 cells were transfected with p3TP-Lux and either empty vector (Mock) or plasmid vectors expressing HA-Smad3 and/or FLAG-Smad7 and treated with 5 ng/ml of TGF-β1 for 16 h. The cell lysates were subsequently subjected to ChIP with the indicated antibodies and precipitated DNAs were amplified using PCR for the 3TP promoter. A control western blot of the transfected cells is shown at the bottom (IB). (**d**) ZEB1 recruits the Smad3/p300 complex to the 3TP-Lux promoter. HepG2 cells were co-transfected with the expression vectors for HA-Smad3, FLAG-Smad7 and/or ZEB1, and p3TP-Lux plasmid and treated with 5 ng/ml of TGF-β1 for 16 h. The cell lysates were analyzed using ChIP. After immunoprecipitation with each indicated antibody, the 3TP promoter region was amplified by PCR using specific primers. A control western blot of the transfected cells is also shown. (**e**) Ectopic expression of ZEB1 causes efficient recruitment of the Smad3/p300 complex to the 3TP-Lux promoter in HTLV-1 (+) cell lines. MT2 cells were transfected with p3TP-Lux and either empty vector (Mock) or *ZEB1* expression vector and treated with 10 ng/ml of TGF-β1 for 24 h. The cell lysates were subjected to ChIP analysis with the indicated antibodies and primers specific for the 3TP promoter. A western blot of the transfected cells is shown in the left panel.

p3TP-Lux and *ZEB1* expression plasmids (Figure 5e). In the absence of TGF-β1, Smad7, ZEB1 and HDAC1 were detected on the 3TP promoter region; however, recruitment of Smad3 and p300 were detected along with a decrease of HDAC1 binding after TGF-β1 treatment. In Mock-transfected cells, protein complex of Smad7 and HDAC1 bound to the 3TP promoter region regardless of TGF-β1 treatment. To assess the possibility that ZEB1 might interfere with the interaction between Smad7 and HDAC1, we co-transfected GFP-Smad7 and FLAG-HDAC1 expression plasmids with increasing amounts of the *ZEB1* expression plasmid and subjected to co-immunoprecipitation using the anti-GFP antibody (Supplementary Figure 10). The HDAC1/Smad7 complex was clearly detected in the absence of ZEB1 transfection; however, the level of the HDAC1/Smad7 complex was decreased when increasing amounts of the *ZEB1* expression vector were transfected with both the GFP-Smad7 and FLAG-HDAC1 expression plasmids. These results suggest that ZEB1 recruits the Smad3/p300 complex to the 3TP promoter with the activation of TGF-β1 signal transduction despite the presence of Smad7 on the 3TP promoter region.

ZEB1 *expression extended the duration of* PAI-1 *and* p21 *transcriptional activation by TGF-β1 signaling in lymphoid cells*

The expression of I-Smads is quickly induced upon stimulation by TGF-β, and I-Smads may be part of the negative feedback control mechanism. We used semiquantitative RT–PCR to initially determine the expression pattern of ZEB1 and ZEB2, members of the zinc-finger E-box binding homeobox protein (ZFHX) family, in various hematopoietic cell populations. ZEB1 was expressed in the B- and T-cell populations in the spleen and the $CD4^+CD8^+$ DP, $CD4^+$ SP and $CD8^+$ SP T cells in the thymus (Figure 6a); however, ZEB2 was weakly expressed in the B-cell fraction in the spleen. Therefore, ZEB1 appears to have an important role in the late stages of T-cell development. To examine how *ZEB1* expression modulates TGF-β1 signaling, we used the murine interleukin-2 (IL-2)-dependent T-lymphoma cell line CTLL2, which has high expression of ZEB1 and low or no expression of Smad7, for this experiment. CTLL2 is known to be one of the T-cell lines that is highly responsive the treatment of TGF-β1, showing a decrease in cell viability to approximately 40%, compared to the control 2 days after TGF-β1 stimulation (Inge *et al*., 1992; Hidaka *et al*., 2008). To investigate the role that ZEB1 has in TGF-β1 signaling in CTLL2 cells, we transfected the cells with a ZEB1 shRNA vector (CTLL2-shZEB1) or a luciferase shRNA vector, which served as a control (CTLL2-shLuc), and examined the TGF-β1-induced transcription of *Smad6*, *Smad7*, *PAI-1* and *p21* by semiquantitative and quantitative RT–PCR. As previously reported, survival rates of CTLL2-shZEB1 cells increased to 60% after treatment with TGF-β1 (data not shown, Hidaka *et al*., 2008). As shown in Figure 6b, treatment of TGF-β1 immediately induced *Smad6* and *Smad7* transcription as early as 30 min, and *PAI-1* mRNA was induced 1 h after TGF-β1 treatment. Peak expression of *PAI-1* mRNA in parental and CTLL2-shLuc cells continued for 12 h and then decreased to background levels 24 h after TGF-β1 treatment (Figure 6b). Similarly, in CTLL2-shZEB1 cells, *PAI-1* mRNA was induced 1 h after TGF-β1 treatment with a similar level of *PAI-1* mRNA as in control cells. However, the downregulation of *PAI-1* mRNA began as early as 4 h and continued to decrease to background levels at 12 h after TGF-β1 treatment (top, Figure 6c). Conversely, the expression of *p21* mRNA started to increase at 4 h after TGF-β1 treatment, whereas the peak was half that of control CTLL2 cells. Moreover, the highest expression level of *p21* lasted from 4 to 24 h in control cells; whereas that duration was shortened to 4–12 h in CTLL2-shZEB1 cells (bottom, Figure 6c). Thus, *ZEB1* expression in CTLL2 cells extended the duration of TGF-β1 signaling up to 24 h after TGF-β1 treatment. Because the duration of Smad3 phosphorylation in CTLL2-shZEB1 cells was not significantly different from those in the control cells (Supplementary Figure 11), it appears that *ZEB1* expression may enhance TGF-β1 signaling without affecting Smad3 phosphorylation in CTLL2 cells. To confirm the colocalization of ZEB1 and Smad7 in CTLL2 cells, we visualized both proteins by immunofluorescence, at the indicated times, after TGF-β1 treatment. ZEB1 constitutively localized to the nucleus, and Smad7, which was induced after TGF-β1 treatment, was also predominantly localized to the nucleus (Figure 6d). To confirm the protein complex of endogenous Smad3, Smad7 and ZEB1 on the TGF-β1 responsive promoter in CTLL2 cells after TGF-β1 treatment, we used ChIP using the corresponding specific antibody. Protein complex of Smad3, Smad7 and ZEB1 bound to the *p21* promoter in CTLL2 cells 12 h after TGF-β1 stimulation (top, Figure 6e). To confirm that Smad7 directly binds to the SRE in the *p21* promoter region, we constructed *p21* promoter reporter with mutated SRE for analyses of ChIP and the promoter activity induced by TGF-β1 (Seoane *et al*., 2004). The mutated SRE in the *p21* promoter region totally abolished the DNA-binding activity of Smad7 by ChIP analysis (Figure 6f) and the level of the promoter activity was significantly reduced after TGF-β1 stimulation (Supplementary Figure 12), suggesting that Smad7 directly binds to the SRE with recruitment of the Smad3/ZEB1 complex. In MOLT4 cells, Smad7 and ZEB1 associated with the *p21* promoter regardless of TGF-β1 treatment and Smad3 recruitment could be detected upon stimulation with TGF-β1 (bottom, Figure 6e). Furthermore, knockdown of ZEB1 diminished the recruitment of Smad3 to the protein complex on the *p21* promoter in CTLL2 cells (Figure 6g), thus suggesting that ZEB1 was necessary for keeping Smad3 in the protein complex on the *p21* promoter with SRE to elongate the active status of TGF-β1 signaling. Figure 7a illustrates a model for the ZEB1-dependent transcriptional control in the TGF-β1 signaling pathway in CTLL2 cells. As a negative feedback mechanism, the expression of *Smad7* is induced within 1 h of TGF-β1

stimulation by Smad signal transduction pathways. The phosphorylated Smad3 cooperates with p300 and ZEB1 to activate many cellular genes within 1–12 h after TGF-β1 stimulation, including *PAI-1* and *p21*, through its ability to interact with several transcription factors, even though Smad7 protein accumulates in the cells at the later stages of development. When *ZEB1* expression was down-regulated by transfection with shZEB1, phosphorylated Smad3 could not bind to the *p21* promoter with SRE, which due to Smad7 interference, and *p21* transcription is shut off 4–12 h after TGF-β1 stimulation (Figure 7b). In the MOLT4 cell line, high expression of ZEB1 recruits phosphorylated Smad3 complex to the *p21* promoter region with the constitutive expression of Smad7, and weakly maintains TGF-β1 signaling with a survival rate of approximately 70% (Figure 7c). In HTLV-1 (+) cells, constitutive binding of Smad7 protein to the *p21* promoter region with SRE interferes with phosphorylated Smad3 complex to block TGF-β1 signaling, and most of the HTLV-1 (+) cells could survive after TGF-β1 treatment (Figure 7d).

Discussion

In this report, we showed that TGF-β signaling is enhanced by ZEB1, which binds to both R-Smads and I-Smads. Transcription of inhibitory I-Smad6 and I-Smad7 is immediately induced by the binding of

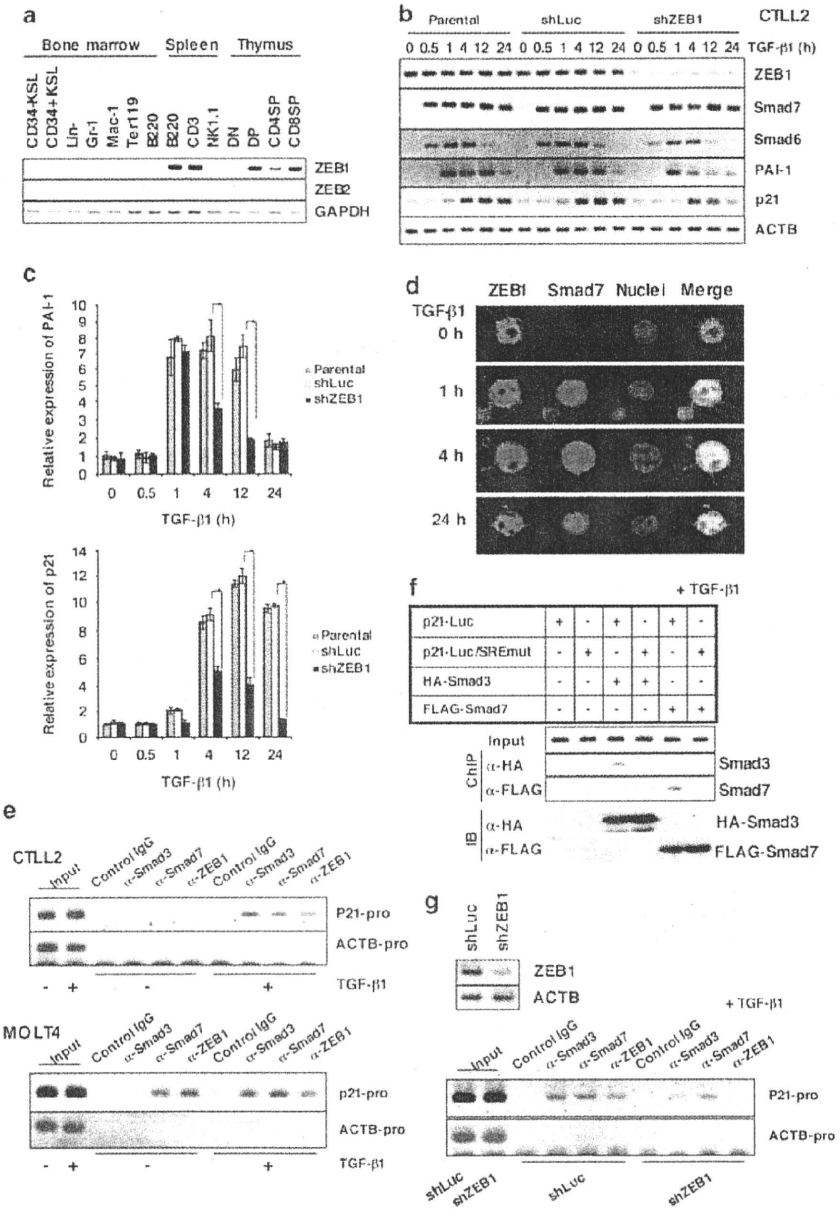

phosphorylated R-Smads to the promoter of Smad6 and Smad7 after TGF-β signaling. TGF-β signaling is suppressed by I-Smads in a negative feedback mechanism. In lymphoid cells, Smad7 is localized on the promoter with the SREs in the nucleus to suppress TGF-β signaling following induction of TGF-β; however, ZEB1 recruits the phosphorylated R-Smad complex to the promoter and enhances TGF-β signaling. Thus, ZEB1 may have important roles in the regulation of TGF-β1 signaling by binding to R-Smads and I-Smads. Moreover, while analyzing the molecular mechanism of resistance to TGF-β signaling in ATLL, we identified that both ZEB1 downregulation and Smad7 overexpression contribute to the TGF-β resistance.

Several reports have described the mechanism by which I-Smads inhibit TGF-β1 signaling. I-Smads located in the cytoplasm have been reported to bind TGF-β type I receptors, recruit E3 ubiquitin ligases (Smurfs) to type I receptors or bind to phosphorylated Smad1 and inhibit the formation of the R-Smad/Co-Smad complex (Hata *et al*., 1998; Souchelnytskyi *et al*., 1998; Kavsak *et al*., 2000; Ebisawa *et al*., 2001). Conversely, I-Smads

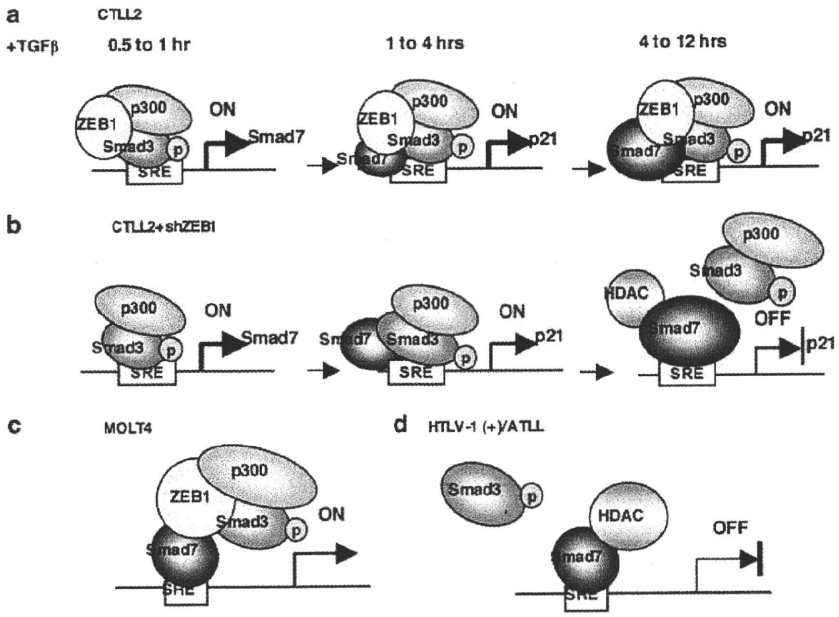

Figure 7 Schematic models for Smad-dependent transcriptional repression and transcriptional activation complexes on SRE in various kinds of cell lines. (**a**) CTLL2; (**b**) CTLL2 transfected with shZEB1; (**c**) MOLT4, T-ALL cell line and (**d**) HTLV-1 (+)/ATLL cells. See text for details.

Figure 6 ZEB1 regulates the duration of Smad-dependent transcription. (**a**) Semiquantitative RT–PCR analysis of *ZEB1* and *ZEB2* mRNA expression was performed with mRNA isolated from $CD34^-$ KSL cells, $CD34^+$ KSL cells, lineage $marker^-$ cells, $Gr\text{-}1^+$ neutrophils, $Mac\text{-}1^+$ monocytes/macrophages, $TER119^+$ erythroblasts and $B220^+$ B lymphoid cells from the bone marrow, $B220^+$ B lymphoid cells, $CD3^+$ T lymphoid cells and $NK\text{-}1.1^+$ natural killer cells from the spleen. In addition, mRNA was isolated from $CD4^-CD8^-$, $CD4^+CD8^+$, $CD4^+CD8^-$ and $CD4^-CD8^+$ T-lymphoid cells from the thymus of adult mice. The expression of glyceraldehyde-3-phosphate dehydrogenase (*GAPDH*) is shown at the bottom as a control. (**b**) CTLL2 cells were untransfected (Parental) or transfected with the control luciferase-specific shRNA vector (shLuc), or the ZEB1-specific shRNA vector (shZEB1) and then treated with 10 ng/ml of TGF-β1. Total RNA was isolated at the indicated time points and semiquantitative RT–PCR was performed with specific primers for *ZEB1*, *Smad6*, *Smad7*, *PAI-1*, *p21* and β-actin. (**c**) Quantitative real-time PCR analysis of *PAI-1* (top) and *p21* (bottom) mRNA expression in the same conditioned CTLL2 cell lines as **b**. Student's *t*-test was used for the statistical analysis, and $P<0.05$ (asterisk) was considered significant. (**d**) Subcellular localization of ZEB1 and Smad7 in the CTLL2 cell lines at the indicated time periods after treatment with 10 ng/ml of TGF-β1. The localization of endogenous ZEB1 and Smad7 was detected by indirect immunofluorescence using an anti-ZEB1 (green, Alexa Fluor 488) and anti-Smad7 antibody (red, Alexa Fluor 555) using the same strategy as described in Figure 3. The cells were analyzed by confocal microscopy, and a DAPI (4,6-diamidino-2-phenylindole) stain was used to visualize the position of the nuclei (blue). (**e**) Protein complex of Smad3, Smad7 and ZEB1 bound to the *p21* promoter after TGF-β1 treatment. Chromatin from CTLL2 (top) and MOLT4 (bottom) cells treated with or without 10 ng/ml of TGF-β1 for 12 h was immunoprecipitated with antibodies against Smad3, Smad7, ZEB1 or normal rabbit serum (as negative controls) and immunoprecipitated DNA was analyzed by PCR using the indicated primer pairs. PCR using primers specific for the β-actin (*ACTB*) promoter was included for the specificity of the ChIP assay. (**f**) CTLL2 cells were co-transfected with a p21-Luc or p21-Luc/SREmut reporter construct and/or expression vectors for either HA-Smad3 or FLAG-Smad7 and treated with 10 ng/ml of TGF-β1 for 12 h. The cell lysates were analyzed using ChIP. A control western blot of the transfected cells is also shown. (**g**) Occupancy of Smad3 is reduced in the protein complex on the *p21* promoter with SRE in CTLL2-shZEB1 cells. CTLL2 cells were transfected with the control shRNA vector (shLuc), or the ZEB1-specific shRNA vector (shZEB1) and treated with 10 ng/ml of TGF-β1 for 12 h. The cell lysates were analyzed using ChIP. Semiquantitative RT–PCR for *ZEB1* and β-actin mRNA are shown at the top panel.

that reside in the nucleus interact with the transcriptional co-repressors Hoxc-8 or CtBP to inhibit BMP-induced transcription or bind to DNA to competitively inhibit the formation of the Smad/DNA complex (Bai *et al.*, 2000; Lin *et al.*, 2003; Zhang *et al.*, 2007). In ATLL cells, Smad7 predominantly localizes to the nucleus and binds to the promoter region of TGF-β1 responsive genes with SRE to inhibit formation of the R-Smad/DNA complex. The differential localization of Smad7 between cell types is currently unknown; however, Smurf-mediated nuclear export of Smad7 has been shown in several studies (Kavsak *et al.*, 2000; Suzuki *et al.*, 2002). In our study using DNA microarrays, we found that the expression level of Smurf1 in acute-type ATLL cells was higher than in $CD4^+$ T lymphocytes from normal volunteers; however, the expression of Smurf2 was lower in ATLL cells (data not shown). Therefore, further studies are needed to clarify the mechanism of Smad7 nuclear localization in ATLL cells.

I-Smads have important roles in the negative feedback mechanism of Smad signaling, and protein phosphatase 1A was recently identified as a Smad phosphatase that terminates TGF-β1 signaling (Lin *et al.*, 2006). Protein phosphatase 1A enhances the disassembly of the activated Smad complex by dephosphorylation of TGF-β1-activated Smad2/3 and promotes nuclear export of dephosphorylated Smad2/3. In T lymphocytes, transcriptional activation by TGF-β1 signaling was terminated within 24 h in both the control CTLL2 and CTLL2-shZEB1 cells, suggesting that protein phosphatase 1A terminates TGF-β1 signaling within 24 h. However, expression of ZEB1 in CTLL2 cells elongated the duration of TGF-β1-induced transcriptional activation of *PAI-1* and *p21* to overcome the suppressor activity of I-Smad6 and I-Smad7 until 24 h. Therefore, we speculate that the elongation of TGF-β1 signaling by ZEB1 is necessary for suppression of the cell growth of T lymphocytes during T-cell differentiation by TGF-β1.

In this study, we showed that ZEB1 interacts with both R-Smads and I-Smads to enhance TGF-β1 signaling and counteracts the Smad7-mediated inhibition of TGF-β1 signaling. We showed that ZEB1 is specifically expressed in $CD4^+CD8^+$ DP lymphocytes through $CD4^+$ SP T lymphocytes (Figure 6a), and *ZEB-1*-deficient mice frequently develop $CD4^+$ T-lymphoma/leukemia (Hidaka *et al.*, 2008). This suggests that the expression of ZEB1 during the late stages of T-cell differentiation is necessary for enhancing the growth-inhibitory effect of TGF-β1 on $CD4^+$ T cells. In addition, recent studies have shown that in Sézary syndrome, an aggressive cutaneous T-cell lymphoma/leukemia, genomic deletion of *ZEB1* has been detected in approximately half of patients (Vermeer *et al.*, 2008). Although Smad7 overexpression has not yet been reported in Sézary syndrome, downregulation of ZEB1, in combination with Smad7 overexpression, may be an important event for the development of peripheral types of T-cell leukemia/lymphoma.

Materials and methods

Cell lines

MOLT4, MKB1, KAWAI and Jurkat are HTLV-1-negative human T-ALL cell lines (Schneider *et al.*, 1977). MT2 and Hut102 are HTLV-1-infected T-cell lines with polyclonal viral integration (Miyoshi *et al.*, 1981). KOB, SO4 and KK1 are IL-2-dependent ATLL cell lines (Yamada *et al.*, 1996). ED and S1T are IL-2-independent ATLL cell lines (Okada *et al.*, 1985). In this report, both the HTLV-1-infected cell lines and ATLL-derived cell lines were referred to as HTLV-1-positive cell lines. CTLL2 is an IL-2-dependent murine cytotoxic T-cell line (Gillis and Smith, 1977). These cell lines were maintained in RPMI 1640 medium (Invitrogen, Carlsbad, CA, USA) supplemented with 10% fetal calf serum (FCS), either with or without IL-2. HEK293T (human embryonic kidney) and HepG2 (human hepatocellular carcinoma) cells were cultured in Dulbecco's modified Eagle's medium (Invitrogen) with 10% fetal calf serum.

Conflict of interest

The authors declare no conflict of interest.

Acknowledgements

This work was supported by Grants-in-Aid for Scientific Research of Priority Area from the Ministry of Education, Culture, Sports, Science and Technology, Japan; Leukemia Research fund; Research fund from Miyazaki Prefecture Collaboration of Regional Entities for the Advancement of Technological Excellence, JST (KM) and Young Scientists (B) (19790344) of Japan Society for the Promotion of Science (SN).

References

Arnulf B, Villemain A, Nicot C, Mordelet E, Charneau P, Kersual J *et al.* (2002). Human T-cell lymphotropic virus oncoprotein Tax represses TGF-beta 1 signaling in human T cells via c-Jun activation: a potential mechanism of HTLV-I leukemogenesis. *Blood* **100**: 4129–4138.

Bai S, Shi X, Yang X, Cao X. (2000). Smad6 as a transcriptional corepressor. *J Biol Chem* **275**: 8267–8270.

Blobe GC, Schiemann WP, Lodish HF. (2000). Role of transforming growth factor β in human disease. *N Engl J Med* **342**: 1350–1358.

Derynck R, Akhurst RJ, Balmain A. (2001). TGF-beta signaling in tumor suppression and cancer progression. *Nat Genet* **29**: 117–129.

Ebisawa T, Fukuchi M, Murakami G, Chiba T, Tanaka K, Imamura T *et al.* (2001). Smurf1 interacts with transforming growth factor-beta type I receptor through Smad7 and induces receptor degradation. *J Biol Chem* **276**: 12477–12480.

Gillis S, Smith KA. (1977). Long term culture of tumour-specific cytotoxic T cells. *Nature* **268**: 154–156.

Hata A, Lagna G, Massagué J, Hemmati-Brivanlou A. (1998). Smad6 inhibits BMP/Smad1 signaling by specifically competing with the Smad4 tumor suppressor. *Genes Dev* **12**: 186–197.

Hidaka T, Nakahata S, Hatakeyama K, Hamasaki M, Yamashita K, Kohno T *et al.* (2008). Down-regulation of TCF8 is involved in the

leukemogenesis of adult-T cell leukemia/lymphoma. *Blood* **112**: 383–393.

Inge TH, McCoy KM, Susskind BM, Barrett SK, Zhao G, Bear HD. (1992). Immunomodulatory effects of transforming growth factor-beta on T lymphocytes. Induction of CD8 expression in the CTLL-2 cell line and in normal thymocytes. *J Immunol* **148**: 3847–3856.

Kavsak P, Rasmussen RK, Causing CG, Bonni S, Zhu H, Thomsen GH *et al.* (2000). Smad7 binds to Smurf2 to form an E3 ubiquitin ligase that targets the TGF beta receptor for degradation. *Mol Cell* **6**: 1365–1375.

Kim SJ, Kehrl JH, Burton J, Tendler CL, Jeang KT, Danielpour D *et al.* (1990). Transactivation of the transforming growth factor beta 1 (TGF-beta 1) gene by human T lymphotropic virus type 1 tax: a potential mechanism for the increased production of TGF-beta 1 in adult T cell leukemia. *J Exp Med* **172**: 121–129.

Kingsley DM. (1994). The TGF-beta superfamily: new members, new receptors, and new genetic tests of function in different organisms. *Genes Dev* **8**: 133–146.

Lin X, Duan X, Liang YY, Su Y, Wrighton KH, Long J *et al.* (2006). PPM1A functions as a Smad phosphatase to terminate TGFbeta signaling. *Cell* **125**: 915–928.

Lin X, Liang YY, Sun B, Liang M, Shi Y, Brunicardi FC *et al.* (2003). Smad6 recruits transcription corepressor CtBP to repress bone morphogenetic protein-induced transcription. *Mol Cell Biol* **23**: 9081–9093.

Miyoshi I, Kubonishi I, Yoshimoto S, Akagi T, Ohtsuki Y, Shiraishi Y *et al.* (1981). Type C virus particles in a cord T-cell line derived by co-cultivating normal human cord leukocytes and human leukaemic T cells. *Nature* **294**: 770–771.

Mochizuki N, Shimizu S, Nagasawa T, Tanaka H, Taniwaki M, Yokota J *et al.* (2000). A novel gene, MEL1, mapped to 1p36.3 is highly homologous to the MDS1/EVI1 gene and is transcriptionally activated in t(1;3)(p36;q21)-positive leukemia cells. *Blood* **96**: 3209–3214.

Mori N, Morishita M, Tsukazaki T, Giam CZ, Kumatori A, Tanaka Y *et al.* (2001). Human T-cell leukemia virus type I oncoprotein Tax represses Smad-dependent transforming growth factor beta signaling through interaction with CREB-binding protein/p300. *Blood* **97**: 2137–2144.

Okada M, Maeda M, Tagaya Y, Taniguchi Y, Teshigawara K, Yoshiki T *et al.* (1985). TCGF (IL 2)-receptor induction Factor (S). II. Possible role of ATL-derived factor (ADF) on constitutive IL 2 receptor expression of HTLV-1(+) T cell lines. *J Immunol* **135**: 3995–4003.

Postigo AA. (2003). Opposing functions of ZEB proteins in the regulation of the TGFbeta/BMP signaling pathway. *EMBO J* **22**: 2443–2452.

Schneider U, Schwenk HU, Bornkamm G. (1977). Characterization of EBV-genome negative 'null' and 'T' cell lines derived from children with acute lymphoblastic leukemia and leukemic transformed non-Hodgkin lymphoma. *Int J Cancer* **19**: 621–626.

Shi Y, Massagué J. (2003). Mechanisms of TGF-beta signaling from cell membrane to the nucleus. *Cell* **113**: 685–700.

Seoane J, Le HV, Shen L, Anderson SA, Massagué J. (2004). Integration of Smad and forkhead pathways in the control of neuroepithelial and glioblastoma cell proliferation. *Cell* **117**: 211–223.

Souchelnytskyi S, Nakayama T, Nakao A, Morén A, Heldin CH, Christian JL *et al.* (1998). Physical and functional interaction of murine and Xenopus Smad7 with bone morphogenetic protein receptors and transforming growth factor-beta receptors. *J Biol Chem* **273**: 25364–25370.

Suzuki C, Murakami G, Fukuchi M, Shimanuki T, Shikauchi Y, Imamura T *et al.* (2002). Smurf1 regulates the inhibitory activity of Smad7 by targeting Smad7 to the plasma membrane. *J Biol Chem* **277**: 39919–39925.

Tsukasaki K, Krebs J, Nagai K, Tomonaga M, Koeffler HP, Bartram CR *et al.* (2001). Comparative genomic hybridization analysis in adult T-cell leukemia/lymphoma: correlation with clinical course. *Blood* **97**: 3875–3881.

van Grunsven LA, Schellens A, Huylebroeck D, Verschueren K. (2001). SIP1 (Smad interacting protein 1) and deltaEF1 (delta-crystallin enhancer binding factor) are structurally similar transcriptional repressors. *J Bone Joint Surg Am* **83-A**: Suppl 1 (Part 1): S40–S47.

Vermeer MH, van Doorn R, Dijkman R, Mao X, Whittaker S, van Voorst Vader PC *et al.* (2008). Novel and highly recurrent chromosomal alterations in Sézary syndrome. *Cancer Res* **68**: 2689–2698.

Yamada Y, Ohmoto Y, Hata T, Yamamura M, Murata K, Tsukasaki K *et al.* (1996). Features of the cytokines secreted by adult T cell leukemia (ATL) cells. *Leuk Lymphoma* **21**: 443–447.

Yasunaga J, Matsuoka M. (2003). Leukemogenesis of adult T-cell leukemia. *Int J Hematol* **78**: 312–320.

Yoshida M, Nosaka K, Yasunaga J, Nishikata I, Morishita K, Matsuoka M. (2004). Aberrant expression of the MEL1S gene identified in association with hypomethylation in adult T-cell leukemia cells. *Blood* **103**: 2753–2760.

Zhang S, Fei T, Zhang L, Zhang R, Chen F, Ning Y *et al.* (2007). Smad7 antagonizes transforming growth factor beta signaling in the nucleus by interfering with functional Smad-DNA complex formation. *Mol Cell Biol* **27**: 4488–4499.

Supplementary Information accompanies the paper on the Oncogene website (http://www.nature.com/onc)

VOLUME 28 · NUMBER 9 · MARCH 20 2010

JOURNAL OF CLINICAL ONCOLOGY ORIGINAL REPORT

Phase I Study of KW-0761, a Defucosylated Humanized Anti-CCR4 Antibody, in Relapsed Patients With Adult T-Cell Leukemia-Lymphoma and Peripheral T-Cell Lymphoma

Kazuhito Yamamoto, Atae Utsunomiya, Kensei Tobinai, Kunihiro Tsukasaki, Naokuni Uike, Kimiharu Uozumi, Kazunari Yamaguchi, Yasuaki Yamada, Shuichi Hanada, Kazuo Tamura, Shigeo Nakamura, Hiroshi Inagaki, Koichi Ohshima, Hitoshi Kiyoi, Takashi Ishida, Kouji Matsushima, Shiro Akinaga, Michinori Ogura, Masao Tomonaga, and Ryuzo Ueda

From Department of Hematology and Cell Therapy, Aichi Cancer Center; Department of Clinical Pathophysiology and Department of Infectious Diseases, Nagoya University Graduate School of Medicine; Department of Hematology and Oncology, Nagoya Daini Red Cross Hospital, Nagoya; Department of Clinical Pathology and Department of Medical Oncology and Immunology, Nagoya City University Graduate School of Medical Sciences, Nagaya; Department of Hematology, Imamura Bun-in Hospital; Department of Internal Medicine, National Hospital Organization Kagoshima Medical Center; Department of Hematology and Immunology, Kagoshima University Hospital, Kagoshima; Hematology and Stem Cell Transplantation Division, National Cancer Center Hospital; Department of Safety Research on Blood and Biologics, National Institute of Infectious Diseases; Department of Molecular Preventive Medicine, Graduate School of Medicine, The University of Tokyo; Kyowa Hakko Kirin Co Ltd, Tokyo; Department of Hematology and Molecular Medicine Unit and Department of Laboratory Medicine, Nagasaki University Graduate School of Biomedical Science, Nagasaki; Department of Hematology, National Kyushu Cancer Center; The Department of Medicine, Division of Medical Oncology, Infectious Disease, and Endocrinology, School of Medicine, Fukuoka University, Fukuoka; and the Department of Pathophysiology, Kurume University School of Medicine, Kurume, Japan.

Submitted July 27, 2009; accepted November 16, 2009; published online ahead of print at www.jco.org on February 22, 2010.

Presented in part at the 50th Annual Meeting of the American Society of Hematology, San Francisco, CA, December 6-9, 2008.

Authors' disclosures of potential conflicts of interest and author contributions are found at the end of this article.

Clinical Trials repository link available on JCO.org.

Corresponding author: Kazuhito Yamamoto, MD, PhD, Department of Hematology and Cell Therapy, Aichi Cancer Center, 1-1 Kanokoden, Chikusa-ku, Nagoya, Aichi 464-8681, Japan; e-mail: kyamamoto@aichi-cc.jp.

0732-183X/10/2809-1591/$20.00

DOI: 10.1200/JCO.2009.25.3575

ABSTRACT

Purpose
KW-0761, a defucosylated humanized anti-CC chemokine receptor 4 (CCR4) antibody, exerts a strong antibody-dependent cellular cytotoxic effect. This phase I study assessed the safety, pharmacokinetics, recommended phase II dose and efficacy of KW-0761 in patients with relapsed CCR4-positive adult T-cell leukemia-lymphoma (ATL) or peripheral T-cell lymphoma (PTCL).

Patients and Methods
Sixteen patients received KW-0761 once a week for 4 weeks by intravenous infusion. Doses were escalated, starting at 0.01, 0.1, 0.5, and finally 1.0 mg/kg by a 3 + 3 design.

Results
Fifteen patients completed the protocol treatment. Only one patient, at the 1.0 mg/kg dose, developed grade 3 dose-limiting toxicities, skin rash, and febrile neutropenia, and grade 4 neutropenia. Other treatment-related grade 3 to 4 toxicities were lymphopenia (n = 10), neutropenia (n = 3), leukopenia (n = 2), herpes zoster (n = 1), and acute infusion reaction/cytokine release syndrome (n = 1). Neither the frequency nor severity of toxicities increased with dose escalation. The maximum tolerated dose was not reached. Therefore, the recommended phase II dose was determined to be 1.0 mg/kg. No patients had detectable levels of anti-KW-0761 antibody. The plasma maximum and trough, and the area under the curve of 0 to 7 days of KW-0761, tended to increase dose and frequency dependently. Five patients (31%; 95% CI, 11% to 59%) achieved objective responses: two complete (0.1; 1.0 mg/kg) and three partial (0.01; 2 at 1.0 mg/kg) responses.

Conclusion
KW-0761 was tolerated at all the dose levels tested, demonstrating potential efficacy against relapsed CCR4-positive ATL or PTCL. Subsequent phase II studies at the 1.0 mg/kg dose are thus warranted.

J Clin Oncol 28:1591-1598. © 2010 by American Society of Clinical Oncology

INTRODUCTION

The successful use of monoclonal antibodies (mAb) has evolved into a promising approach to treating cancer over the last decade. In the field of hematologic malignancies, development of the therapeutic mAb rituximab has changed the standard of therapy for patients with B-cell lymphomas and has markedly improved prognosis.[1-3] In contrast, the prognosis of patients with T-cell neoplasms remains very poor.[4] The 5-year overall survival (OS) for common subtype of peripheral T-cell lymphoma (PTCL), such as PTCL not otherwise specified (NOS) and angioimmunoblastic T-cell lymphoma, is 32% compared with only 14% for adult T-cell leukemia lymphoma (ATL).[4] A recent phase III trial for newly diagnosed aggressive ATL demonstrated that a dose-intensified multidrug chemotherapy with vincristine, cyclophosphamide, doxorubicin, and prednisone (VCAP), doxorubicin, ranimustine, and prednisone (AMP), and vindesine, etoposide, carboplatin, and prednisone (VECP) was more effective than biweekly cyclophosphamide, doxorubicin, vincristine, and prednisone (CHOP).[5] However, the median survival time and OS at 3 years were still unsatisfactory, at approximately 13 months and 24%, respectively.[5,6]

CC chemokine receptor 4 (CCR4) is a chemokine receptor expressed on T-helper type 2[7] and regulatory T cells (Treg).[8-10] Because numerous studies, including our own, have demonstrated CCR4 to be expressed on certain types of T-cell neoplasms,[11-17] we hypothesized that this molecule might represent a novel molecular target for immunotherapy against relapsed or refractory T-cell lymphomas.[16-21] Accordingly, we developed KW-0761, a next generation humanized anti-CCR4 mAb, with a defucosylated Fc region, which markedly enhanced antibody-dependent cellular cytotoxicity (ADCC) due to increased binding affinity to the Fcγ receptor on effector cells.[21,22]

Herein, we report the results of a phase I study designed to assess the safety, pharmacokinetics, recommended phase II dose, and efficacy of KW-0761 in patients with relapsed CCR4-positive ATL and other peripheral T-cell lymphomas (PTCL).

PATIENTS AND METHODS

Investigational Drug and Eligibility

KW-0761 is a defucosylated humanized immunoglobulin G1 (IgG1) l mAb generated from a mouse anti-CCR4 mAb[7] by Kyowa Hakko Kirin Co Ltd.[23,24]

Patients between 20 and 69 years of age with CCR4-positive aggressive ATL (acute type, lymphoma type, or unfavorable chronic type)[25,26] or PTCL with CCR4 expression were eligible. CCR4 expression was confirmed by immunohistochemistry or flow cytometry using an anti-CCR4 mAb (KM2160, Kyowa Hakko Kirin Co Ltd),[12,14,15] and confirmed by the review committee with a central evaluation. Patients with relapse after at least one prior course of chemotherapy were eligible. All patients were required to have an Eastern Cooperative Oncology Group performance status of 0 or 1. Eligibility criteria also included the following laboratory values: an absolute neutrophil count $\geq$ 1,500/uL, platelet count $\geq$ 75,000/uL, hemoglobin $\geq$ 8.0 g/dL, AST $\leq$ 2.5 $\times$ the upper limit of the normal range (UNL), ALT $\leq$ 2.5 $\times$ UNL, total bilirubin $\leq$ 1.5 $\times$ UNL, serum creatinine $\leq$ 1.5 $\times$ UNL, corrected serum calcium $\leq$ 11.0 mg/dL, negative for hepatitis B surface antigen and for hepatitis B virus DNA, and arterial partial oxygen pressure $\geq$ 65 mmHg or arterial blood oxygen saturation $\geq$ 90%. All subjects underwent electrocardiography to confirm the absence of abnormalities requiring treatment and that the left ventricular ejection fraction was at least 50%.

Patients were excluded if they had any severe complication, an infectious complication or active tuberculosis, a history of organ transplantation, active concurrent cancers, CNS involvement, a bulky mass requiring emergent radiotherapy, or tested positive for hepatitis C virus antibody and/or HIV antibody.

The institutional review boards of the participating institutions approved this study, and all patients gave written informed consent according to the Declaration of Helsinki.

Study Design

This was a multicenter dose-escalation study with three to six patients at each dose level to determine the maximum-tolerated dose (MTD) and estimate the recommended phase II dose. Cohorts of patients received KW-0761 at 0.01, 0.1, 0.5, and 1.0 mg/kg, weekly for 4 weeks by intravenous infusion. Premedications (antihistamine and antipyretic) were administered before each KW-0761 treatment.

If no dose-limiting toxicity (DLT) was observed in a cohort of three patients at a given dose level, the next cohort of three new patients would be treated with the next higher dose. If DLT was experienced by one or two of the three patients at any dose, three additional patients would be treated at the same dose level. If three or more patients at a given dose level exhibited DLT, this dose would be considered to exceed the MTD and the dose escalation would thus be halted. The recommended phase II dose was defined as one dose level below the MTD or the maximum dose level judged to be tolerable. An expanded cohort of three additional newly enrolled patients was also treated at the recommended phase II dose. Patients who relapsed after achieving responses to KW-0761 were allowed to be re-treated with this antibody.

Toxicity Evaluation and Definition of DLT

Patients treated at each dose level were evaluated weekly during therapy and until 4 weeks after the last infusion to assess toxicity. Toxicity was graded according to the National Cancer Institute Common Terminology Criteria for Adverse Events version 3. Human anti-KW-0761 antibodies in the plasma of patients were detected by an enzyme-linked immunosorbent assay. The plates were coated with KW-0761 to capture any anti-KW-0761 antibodies, followed by addition of biotinylated KW-0761, and then horseradish peroxidase–labeled avidin. Detection sensitivity of this assay was 5 ng/mL as standard antibody equivalent in plasma.

DLT was defined as an adverse event or a laboratory abnormality that occurred within 28 days after the first infusion, judged to be related to KW-0761 and meeting any of the following criteria: $\geq$ grade 4 hematologic toxicity except lymphopenia, $\geq$ grade 4 symptoms judged to be consistent with an acute infusion reaction/cytokine release syndrome or with tumor lysis

Table 1. Patient Demographic and Clinical Characteristics by Cohort

Characteristic	Cohort and Dosage					Total
	1: 0.01 mg/kg	2: 0.1 mg/kg	3: 0.5 mg/kg	4: 1.0 mg/kg	Expanded: 1.0 mg/kg	
No. of patients	3	4*	3	3	3	16
Median age, years						62
Range	46-68	55-66	60-69	62-64	55-62	46-69
Sex						
Male	2	2	2	0	2	8
Female	1	2	1	3	1	8
Diagnosis						
ATL	2	4	3	2	2	13
PTCL	1 (MF)	0	0	1 (PTCL-NOS)	1 (PTCL-NOS)	3
No. of prior chemotherapy regimens						
1	2	2	2	1	2	9
2	0	0	0	2	0	2
$\geq$ 3	1	2	1	0	1	5

Abbreviations: ATL, adult T-cell leukemia-lymphoma; PTCL, peripheral T-cell lymphoma; NOS, not otherwise specified; MF, mycosis fungoides.
*One patient enrolled at 0.1 mg/kg was withdrawn due to early progressive disease.

syndrome, and ≥ grade 3 nonhematologic toxicities. The independent data monitoring committee evaluated the safety data at all dose levels.

Responses

Responses were evaluated within 2 weeks and again at 4 weeks after the last KW-0761 infusion. The antitumor effects were determined according to criteria described previously.[26,27-29] The overall response (OR) rate included patients with a complete response (CR), CR unconfirmed, or a partial response (PR). Progression-free survival (PFS) was defined from the day of the first KW-0761 infusion until the day of progressive disease (PD) detection or death due to any cause. The tumor response and PFS of each subject were confirmed by the efficacy assessment committee with a central evaluation based on computed tomography imaging.

Pharmacokinetics

Blood was drawn into a heparin-containing tube before and after the infusion in all patients and plasma concentrations of KW-0761 were assessed using an enzyme-linked immunosorbent assay. One blood sample was obtained before each infusion, six during the 0- to 72-hour period after the first or fourth infusion, one immediately after the second or third infusion, and four in the 7 to 28 days after the fourth infusion. The pharmacokinetic parameters of plasma KW-0761 concentrations were calculated by employing a noncompartment model using WINNonlin (Scientific Consulting, Apex, NC) software: plasma maximum (C_{max}) and trough (C_{trough}) drug concentrations after each administration of KW-0761, and the plasma half-life ($t_{1/2}$) and area under the blood concentration time curve ($AUC_{0\text{-}7days}$) after the first and the fourth infusions.

Table 2. Grade 2 or Higher Nonhematologic and Hematologic Adverse Events by Cohort

Adverse Event	Cohort 1 (n = 3)		Cohort 2 (n = 4)		Cohort 3 (n = 3)		Cohort 4 and Expanded (n = 6)	
	Grade 2	Grade 3	Grade 2	Grade 3	Grade 2	Grade 3	Grade 2	Grade 3
Nonhematologic*								
Cardiac arrhythmia and general								
Prolonged QTc	1	—	—	—	—	—	—	—
Vasovagal episode	—	—	—	—	—	—	1†	—
Hypertension	—	—	—	—	—	—	1	—
Hypotension	1†	—	—	—	—	—	—	—
Constitutional symptoms								
Fever	—	—	1†	—	—	—	2 (1†)	—
Dermatology/skin								
Pruritus	—	—	—	—	—	—	1	—
Rash	1	—	—	—	—	—	2	1
Gastrointestinal								
Constipation	1	—	—	—	—	—	—	—
Infection								
Febrile neutropenia	—	—	—	—	—	—	—	1
Herpes zoster‡	—	1	—	—	—	—	—	—
Metabolic								
Alkaline phosphatase	—	—	1†	—	—	—	—	—
ALT	—	—	1	1†	—	—	—	—
AST	—	—	—	1†	—	—	—	—
γ-GTP	—	—	—	1†	—	—	—	—
CRP increased	—	—	—	—	—	—	1†	—
Pain								
Lymph node	—	—	—	—	—	—	1	—
Pulmonary/upper respiratory								
Hypoxemia	—	—	2†	—	—	—	1	—
Syndrome								
Acute infusion reaction/cytokine release	1	—	2	1	1	—	2	—

	Cohort 1 (n = 3)			Cohort 2 (n = 4)			Cohort 3 (n = 3)			Cohort 4 (n = 6)		
	Grade 2	Grade 3	Grade 4	Grade 2	Grade 3	Grade 4	Grade 2	Grade 3	Grade 4	Grade 2	Grade 3	Grade 4
Hematologic*												
Leukopenia	1	—	—	1	—	—	2	1	—	1	1	—
Lymphopenia§	1	1	—	1	1	1	1	2	—	1	3	2
Neutropenia	1	—	—	1	1	—	—	1	—	1	—	1
Thrombocytopenia	1	—	—	—	—	—	—	—	—	—	—	—
Eosinophilia	1	—	—	—	—	—	—	—	—	—	—	—

Abbreviations: QTc, corrected QT interval; γ-GTP, γ-glutamyl transpeptidase; CRP, C-reactive protein.
*KW-0761–related adverse events.
†Adverse events observed as the acute infusion reaction/cytokine release syndrome.
‡Observed 2.5 months after the last administration.
§Includes abnormal cells and was excluded from the definition of dose-limiting toxicities.

RESULTS

Patient Characteristics

Sixteen patients (13 ATL, two PTCL-NOS, one mycosis fungoides) were enrolled in this phase I study (Table 1). Patients characteristics both at first presentation and at study entry are listed in Appendix Table A1 (online only). Four patients were enrolled in cohort 2 because one participant (203) withdrew due to PD after receiving the first infusion. The other 15 patients completed the planned treatment. All 16 enrolled patients were evaluated for toxicity and response on an intent-to-treat basis.

Adverse Events and Nonhematologic Toxicities

All adverse events ≥ grade 2 are listed in Table 2.

The grade 3 nonhematologic toxicities were herpes zoster, skin rash, febrile neutropenia, elevations of ALT, AST, and γ-glutamyl transpeptidase (γ-GTP), and acute infusion/cytokine release syndrome (n = 1, each). All other toxicities observed were ≤ grade 2, and there were no grade 4 or grade 5 nonhematologic toxicities. Among the grade 3 toxicities, increases liver transaminases and γ-GTP were judged to be infusion-related toxicity. Neither the frequency nor the severity of toxicities increased with dose escalation. None of our patients had detectable human anti-KW-0761 antibody. Recovery from toxicities was observed in all cases.

Hematologic Toxicities

Lymphopenia occurred in 14 (88%) of the 16 patients: grade 2 or grade 3 in 11 and grade 4 in three. Grade 4 neutropenia, which developed in one patient, was associated with a febrile episode. Other hematologic toxicities were leukopenia, thrombocytopenia, and eosinophilia. These hematologic toxicities, which were ≤ grade 3, occurred at all the dose levels, but were transient. Recovery to normal or baseline levels was eventually seen in all cases.

Infusion-Related Toxicities

As presented in Table 2, seven (44%) of the 16 patients exhibited ≥ grade 2 acute infusion reaction or cytokine release syndrome. In six cases, the severity was grade 2, and in one grade 3. Overall, 14 patients (88%) had such events with a severity of at least grade 1. These adverse events occurred primarily at the first infusion, then became less frequent with subsequent treatments. The common infusion-related events were vasovagal episodes, hypotension, fever, hypoxemia, and elevations of alkaline phosphatase, C-reactive protein (CRP), liver transaminases, and γ-GTP. None of the patients required interruption of antibody infusion due to these toxicities.

Only one patient (201) who developed grade 2 infusion-related toxicities needed steroid administration for his infusion reactions. He was given one dose of 100 mg hydrocortisone with symptomatic improvement. The remaining patients did not need steroids.

Dose Escalation and DLT

In cohort 1, no DLT was observed during the DLT observation period, although one patient (102) developed grade 3 herpes zoster 2.5 months after the last infusion. This adverse event was treated with topical dressing by ointment and acyclovir and resolved in 1 week. Another patient (103) in cohort 1 showed a grade 3 increase in liver transaminase due to hepatitis B virus reactivation (grade 2) 6 months after the last infusion. At the onset, this patient was receiving the second course of KW-0761 because of PD after achieving PR with the first course, according to the protocol. This event resolved with the antiviral drug entecavir. This event was not judged to represent DLT by the independent data monitoring committee. In cohort 2, one patient (203) showed grade 3 liver function impairment. The event was not, however, considered to represent DLT, instead being judged to be an acute infusion reaction and cytokine syndrome toxicity. Patients in cohorts 3 and 4 developed neither grade 3 nonhematologic or grade 4 hematologic toxicities, nor acute infusion reaction and cytokine syndrome toxicities. Therefore, the MTD was not reached by cohort 4 and the maximum dose of 1.0 mg/kg was thus selected as the dose for the expanded cohort. In the expanded cohort, one patient (412) exhibited grade 4 neutropenia and grade 3 skin rash and febrile neutropenia (Appendix Fig A1, online only), possibly related to KW-0761 treatment. In total, one of the six patients at the 1.0 mg/kg dose level showed a DLT. Taking all data into account, the recommended phase II dose was determined to be 1.0 mg/kg.

Pharmacokinetics

KW-0761 exhibited dose-proportional pharmacokinetics. The plasma C_{max} and C_{trough} as well as the $AUC_{0\text{-}7days}$ increased dose and frequency dependently, as presented in Figure 1 and Table 3. At 1.0 mg/kg, the mean values (± standard deviation [SD]) of C_{max}, C_{trough}, and $AUC_{0\text{-}7days}$ after the first infusion were 21,758 ± 3,495 ng/mL, 7,544 ± 3,009 ng/mL, and 1,879,383 ± 464,447 ng × hours/mL, respectively, while the corresponding values after the fourth infusion were 41,374 ± 5,317 ng/mL, 19,637 ± 3,826 ng/mL, and 4,224,459 ± 533,158 ng × hours/mL. The $t_{1/2}$ was prolonged at the 0.5 and 1.0 mg/kg dose levels as compared with lower doses. The mean value ± SD of $t_{1/2}$ after the fourth infusion at 1.0 mg/kg was 438 ± 76 hours (18.3 ± 3.2 days). There were no significant correlations between any of the pharmacokinetic parameters and either the clinical response to treatment or adverse events.

Responses

Five (31%; 95% CI, 11% to 59%) of the 16 enrolled patients achieved objective responses, including two (13%) with CR and three (19%) with PR (Table 4). The two patients achieving CR had acute-type ATL and their CR status was maintained until the last follow-up (12 and 3 months) without subsequent therapy. Two other acute-type

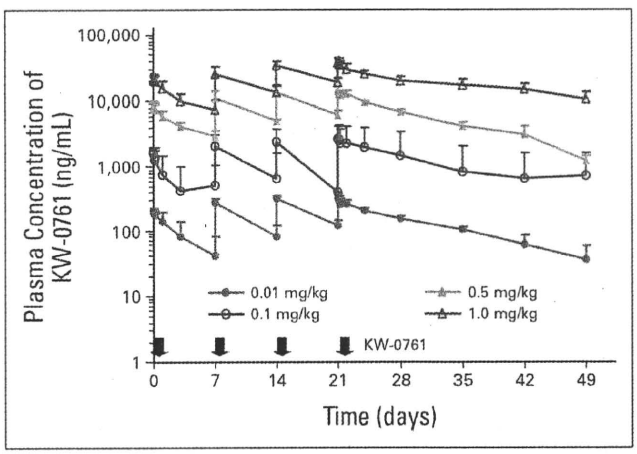

Fig 1. Mean KW-0761 plasma concentration profile by cohort: bar indicates upper limit of standard deviation.

